UNIVERSITÀ DEGLI STUDI DI PADOVA

DEPARTMENT OF GEOSCIENCES
UNIVERSITY OF PADOVA

Master Thesis in Geophysics for natural risks and resources

Seismic Characterization of Subsurface Structure in Enel power plant in Polesine Camerini, Porto Tolle, Italy: A Velocity Model Approach

Master Candidate

MARYAM ABTAHIKASHANI

Student ID 2055574

Supervisor

Prof. Giorgio Cassiani

University of Padova

Co-supervisor

Dr. Alessandro Brovelli

Dr. Gwenola Michaud

Isamgeo S.R.L

Academic Year
2023-2024

Acknowledgments

I want to express my gratitude to my supervisor, Prof. Giorgio Cassiani, for his invaluable guidance and support throughout my master's thesis. His assistance in helping me find a subject of my interest and providing the opportunity to connect with the ISAMGEO company team has been instrumental in the success of this research project.

I am also profoundly grateful to my co-supervisor, Dr. Alessandro Brovelli, who is the CEO of ISAMGEO company. His generosity in allowing me to join the company for a nine-month internship has given me invaluable work experience in a professional environment. I am particularly thankful for his sponsorship of the trips to Porto Tolle for data collection, which enriched my practical understanding and contributed significantly to this study.

My sincere thanks go to my co-supervisor, Dr. Gwenola Michaud, from whom I have learned the most during these past nine months. Her dedication, patience, and willingness to help me overcome numerous challenges have been exceptional. Despite her busy schedule, she always made time to assist me with both the practical work and the writing of this dissertation. Thank you, Gwenola, for your tireless support and mentorship and for the many things that I have learned from you.

It has been a pleasure to work with the ISAMGEO team, and I am thankful for the warm and professional environment they provided.

Lastly, I want to extend my deepest appreciation to Milad, my supportive friend and husband, and to my family and friends, who have always been there for me during the tough times I have gone through. Your encouragement and understanding have been a source of strength for me throughout this journey.

Abstract

Seismic characterization of subsurface structure(s) is a critical component in civil engineering projects, especially for determining soil properties essential for safe and effective construction. This quantitative study investigates the subsurface's seismic properties at the ex-power plant site in Porto Tolle, Italy, aiming to facilitate its transformation into a new, environmentally friendly area. By employing both active and passive seismic data acquisition methods, this research seeks to develop a comprehensive understanding of near-surface soil dynamics and propose a reliable local velocity model for the top-most layer(s).

In this study, we are using both active and passive seismic methods to collect data. Multi-channel analysis of surface waves (MASW) is the active seismic method, and horizontal-to-vertical spectral ratio (H/V) analysis is the passive method used. The primary objective is to estimate the velocity of shear seismic surface waves and characterize the subsurface through dispersion curves and velocity profiles resulting from multi-channel analysis of surface waves. Assessment of the site effects on the amplification of specific frequencies as a function of the local geology and soil characteristics, is the second objective of this study. The study emphasizes the role of passive seismic methods in providing spectral characterization through horizontal-to-vertical spectral ratio analysis, which aids in identifying unique spectral signatures of geological layers.

Results from the multi-offset active acquisitions show that the shear wave velocity is low near the surface and increases with depth, indicating sediment compaction and homogeneity. The absence of significant structural anomalies aligns with findings from H/V analysis and core drilling data reported in another study on the same site (Georicerche, 2024), which show a lack of strong impedance contrasts within the first 50 meters.

In conclusion, this seismic study provides essential data for the redevelopment of the Porto Tolle site, balancing economic development with environmental preservation. The findings support future civil engineering projects by offering detailed insights into near-surface properties, thereby contributing to the region's sustainable growth and risk mitigation strategies.

Table of Contents

1. List of Figures

2. Introduction

Knowledge of the geotechnical properties of subsoil sites is essential in various civil engineering projects. Measurement of dynamic properties, soil thickness, basement depth and its associated in homogeneities such as voids, fractures, joints and shear zones play a very essential part in design and construction of any civil engineering structure. The shear wave velocity of the top-most soil layers is a key parameter in this sense, such as Porto Tolle, Italy. This study provides information to plan the conversion of the ex-power plant site in Porto Tolle, known as the “Enel power plant in Polesine-Camerini”, into a new area with a different application and cleaner activity. It aims to explore the field near-surface soil dynamics characterization with a view to the area rehabilitation. This work is aligned with economic and environmental aspects. The rehabilitation of the ex-power plant is a crucial element for the area's economy.

In recent years, discussions about the future of the Porto Tolle site have continued, with a focus on balancing economic development with environmental preservation. Local authorities and environmental groups advocate for solutions that protect the Po River Delta’s unique ecosystem while providing economic opportunities for the region. Our research provides fundamental information about the field's structural potential, which is essential for future economic investments. Moreover, this study is useful in risk management. The probabilities of any damage or failure of the ex-power plant structures can be detected based on the results of this geophysical project. Estimating the velocity of the seismic surface waves leads us to hypothesize a local velocity model. This analysis is the main objective of this study. It helps us to understand how seismic surface waves propagate through the subsurface during ***active seismic data acquisitions*** and evaluate near-surface properties such as structure. In addition to active seismic data acquisitions for modeling surface wave velocity, the application of ***passive seismic data acquisitions*** cannot be overlooked. One of the primary applications of passive methods is spectral analysis. In environmental and engineering geophysics, spectral analyses play a crucial role in characterizing subsurface properties. By analyzing the frequency content of seismic waves, we can identify the unique spectral signatures of different geological layers and structures, thereby aiding in subsurface mapping. Different geological layers and structures can have distinct spectral signatures.

Spectral characterization, a practical application in seismic data analysis, refers to analyzing a signal's frequency content. It involves examining how the energy or power of seismic waves is distributed across different frequencies. This process can help understand the dominant frequencies present in the seismic data, which can provide insights into the sources and properties of the seismic waves. Spectral characterization can reveal site-specific effects, such as amplification of specific frequencies due to local geology. Finally, comparing the spectra of different signal components (e.g., horizontal vs. vertical components) can provide insights into

wave propagation and site effects, which is the second objective of this study. The "Horizontal - to - Vertical spectral ratio" is used in the site characterization of this project.

This report first provides a literature review of seismic data analysis for near-surface characterization, including the foundation of theory. It then details the location and properties of this empirical research and the methodology applied to estimate the velocity model through multiple analyses of surface waves and spectral analysis. Finally, the results, conclusions, and research gaps are reported.

3. Literature review

3.1. Shear wave velocity

Among all geophysical methods, the seismic method stands out as an efficient tool for determining subsoil characteristics, particularly in areas where subsoil structure is of interest and no fluid dynamics are involved, such as the current case of study. The reason why seismic method is useful for structural characterizations, is that we can study the propagation of seismic waves to retrieve the elastic moduli which are key parameters in the knowledge of the geotechnical properties of subsoil sites. The elastic modulus of each part of the subsoil is a fundamental parameter in estimating the deformation of a structure under different conditions (Lee et al., 2017).

Method	Structure	Dynamic
Seismic	+ +	
Electro-Magnetic	+	++
DC resistivity methods	++	++
Ground Penetration Radar	++	+
Distributed Temp. Sensing		++
Magnetics	+	
Gravimetry	+	+
Spectral Induced Polarization	+	
Self Potential		+
Borehole logs	+ +	+

Table 1: Different applications of geophysical methods (from environmental and engineering geophysics course material, department of geoscience, UNIPD)

In most of the projects similar to this study, the shear modulus is playing the main role rather than other types of elastic modulus such as bulk modulus and Young's modulus. Shear modulus (G), also known as the modulus of rigidity, measures a material's response to shear stress that causes one layer of the material to move parallel to another layer. Shear modulus is given by the formula:

$$G=\frac{\tau}{\gamma}$$

where τ is the shear stress and γ is the shear strain (Chapman, 2004). The shear modulus is retrieved from shear waves or Vs (S-waves). Hence, the study of shear wave velocity of the top-most soil layers is a key parameter in this sense (Olafsdottir et al., 2018).

The relation between the shear wave velocity and the shear modulus is represented as below; where τ is the shear stress and γ is the shear strain. The relation between the shear wave velocity and the shear modulus is represented as below (Foti et al., 2014);

$$Vs = \sqrt{\frac{G}{\rho}}$$

Where Vs is S-wave velocity and ρ is the material density (Chapman, 2004). The estimation of shear wave velocity is essential in assessments of both liquefaction potential and soil amplification and for seismic site classification (Kramer, 1996). Several insitu methods can be applied to estimate near-surface materials' shear wave velocity profiles. We can obtain the Vs models either using the Seismic refraction method with shear wave source and receivers such as borehole methods or using surface wave analysis to retrieve Vs. Borehole methods involving down-hole, cross-hole and seismic cone[1], all need drilled boreholes, which are costly, yet worthy for deeper exploration than near surface.

For surface methods, as noninvasive, done from the surface, we have no need for heavy machinery and boreholes. These methods are environmentally friendly and cost less (Olafsdottir et al., 2018). Among all the surface methods, to observe the near-surface subsoil to a maximum depth of 40 m, we use surface wave seismic method (Socco and &Strobbia, 2004).

3.2. Surface waves seismic

Seismic analyses are categorized into three main branches: refraction seismic, reflection seismic and surface wave seismic. The acoustic waves that are generated from a seismic source in the subsurface are called body waves and are of two types:

[1] seismic cone: a penetro-metric cone equipped with a geophone in the bit and Cautions to the waves travelling along the rods.

i. P-wave with a compressional and longitudinal type of displacement. This wave is called P-wave as it propagates fast and arrives first as a **p**rimary arrival
ii. S-wave with a shear type of displacement. This wave is called S-wave for its shear displacement in the plane perpendicular to the direction of propagation. As it propagates slowly, it arrives as **s**econdary after the P-wave.

When these body waves interfere with the surface, the waves change their displacement along the surface of the earth at the boundary between ground and air. These waves are called surface waves. They are the most energetic waves among all the wave types. Unlike the body waves, they travel in two dimensions and not three.

The relation between surface wave attenuation and the distance from the source is as follows;

$$r^{-0.5}$$

where r is the distance from the source of the wave. For conventional seismic reflection data, surface waves can be considered coherent noise that needs to be eliminated or reduced. Significant efforts have been dedicated to filter out surface waves from reflection data, thereby improving the accurate representation of reflections while disregarding the properties and information content of surface waves.

Recently, there has been a growing interest in the information carried by surface waves. These waves can be interpreted or specifically acquired and analyzed to characterize the shallow near surface. The depth of penetration of the surface waves is roughly equal to one wavelength. (Socco and Strobbia, 2004). The dispersive nature of surface waves in a vertically heterogeneous media includes several different wavelengths in a complex waveform and results in the effect of the surface waves in different depths.

In seismology, there are two main types of surface waves: Rayleigh waves and Love waves. They are distinguished based on the released energy, duration, and motion of the particles in the media through which the waves propagate. Rayleigh waves move in an elliptical motion pattern involving vertical and horizontal ground displacement. These waves typically have lower frequencies and longer wavelengths than body waves (P and S waves). However, Love waves move in a horizontal shearing motion, perpendicular to the direction of wave propagation. They do not have vertical displacement, only horizontal movement. Both Rayleigh and Love waves tend to cause more damage during earthquakes because of their larger amplitudes and longer duration in comparison with the body waves. In Figure 1 and Figure 2, the motion pattern of both Rayleigh and love waves are shown.

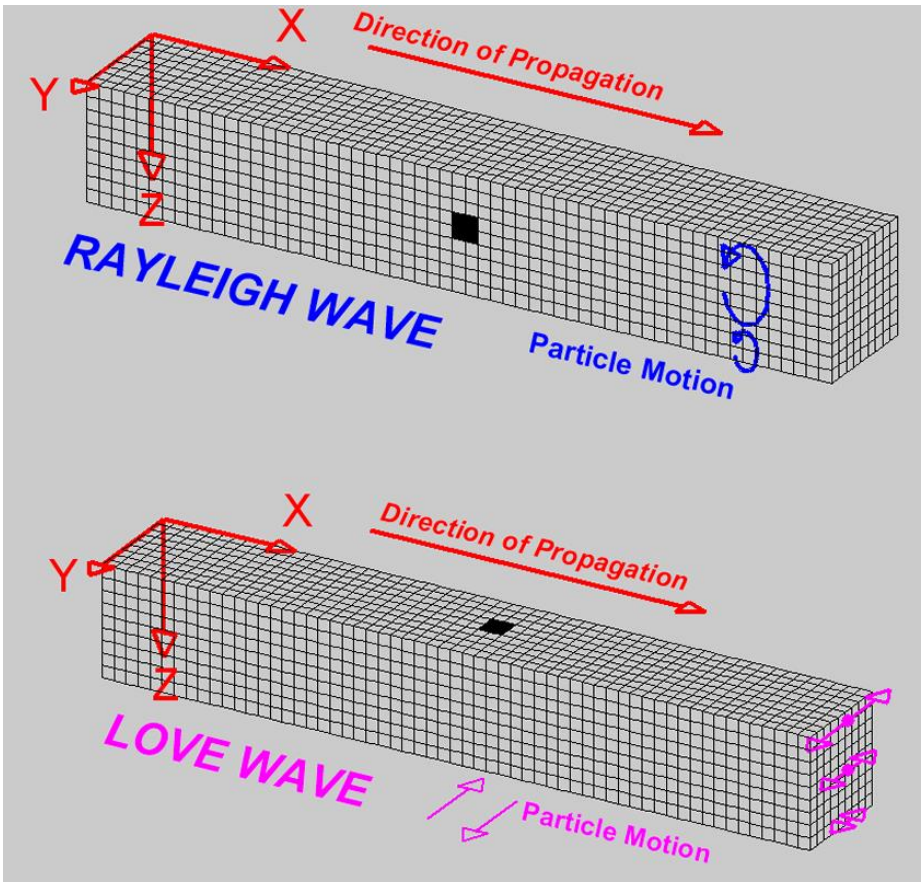

Figure 1: Schematic figure of Rayleigh and Love wave motion patterns (Braile, 2004).

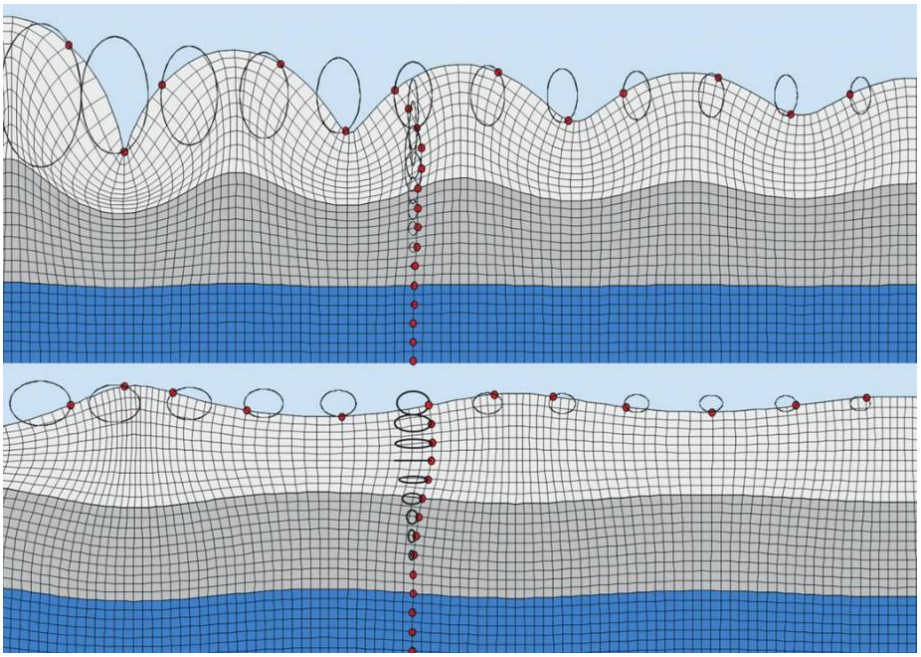

Figure 2: Schematic figure of Rayleigh and Love wave motion patterns (Foti et al., 2014).

The variation of velocity with frequency or wavelength is known as dispersion. In fact, surface waves methods study the dispersion of surface waves propagating through a heterogeneous medium to retrieve (indirectly) the Shear-wave, Vs (Aki and Richards, 1980). The focus has been on the analysis of Rayleigh waves, as they are both easy to generate and to detect on the ground surface using low-frequency receivers (Socco et al., 2010). Rayleigh waves in a homogenous, isotropic media are not dispersive, and their velocity is only a function of the mechanical properties of the media. The frequency dependence of the Rayleigh wave velocity is the result of the phenomenon of geometric dispersion in vertically heterogeneous media (Foti et al., 2014).

In the case of acoustic waves, we deal with two velocities: phase velocity and group velocity. The basis of most surface wave analysis methods is accurately determining the frequency-dependent phase velocity of fundamental-mode Rayleigh waves. Apart from being a function of frequency, the Rayleigh wave phase velocity (V_R) is related to several groups of soil properties, most importantly, the shear wave velocity (Olafsdottir et al., 2018). The velocity of Rayleigh wave is almost equal to the shear wave velocity as follows; $V_R \sim 0.9\ V_S$. In Figure 3, the relations between the Rayleigh wave velocity with the shear wave velocity and the compressional velocity is illustrated. In a homogenous media, the Rayleigh wave is slightly lower than V_S as follows (Socco and Strobbia, 2004):

$$\boldsymbol{0.87\ V_S < V_R < 0.96\ V_S}$$

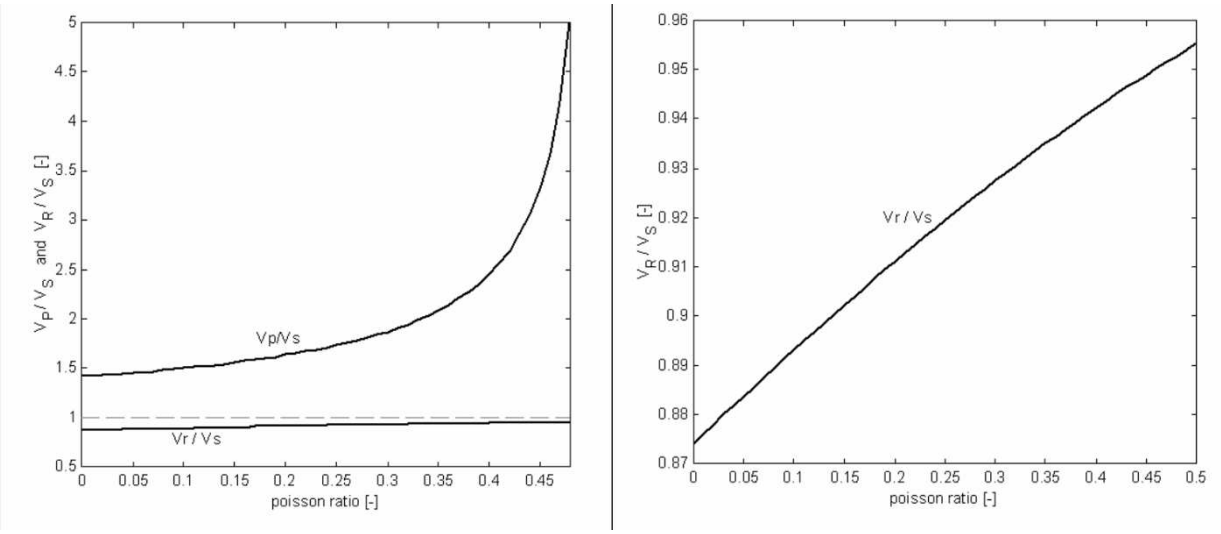

Figure 3: Velocity of Rayleigh waves V_r, compressional wave V_p and shear waves V_s in function of Poisson ratio (from environmental and engineering geophysics course material, department of geoscience, UNIPD).

Before discussing the details of surface wave methods, it is necessary to consider the methods' limitations and uncertainties:

• the depth at which reliable information can be obtained can be limited by the acquisition or the lack of resolution or sensitivity to a specific target.

• most approaches are based on a one-dimensional model.

• the propagation is a multimode phenomenon: the presence of different modes and the modal superposition can introduce ambiguity and complicate the interpretation (Socco and Strobbia, 2004).

3.3. Multichannel analysis of surface waves (MASW) data acquisition and tools

Several geophysical methods have been suggested for characterizing the near surface and measuring shear wave velocity in situ. These methods use various testing configurations, processing techniques, and inversion algorithms. The most commonly used techniques include Spectral Analysis of Surface Waves (SASW) and Multichannel Analysis of Surface Waves (MASW).

SASW technique has been generated by Researchers at the University of Texas, Austin. They introduced a two-receiver approach based on Fast Fourier Transform (FFT) analysis of phase spectra of surface waves generated by an impulsive source such as a sledgehammer, which gained popularity among geotechnical engineers. This approach faced challenges in evaluating and differentiating signals from noise with only a pair of receivers (Gabriels et al., 1987).

In the early 1980s, investigators in the Netherlands used a 24-channel acquisition system to analyze recorded surface waves and deduce the shear-wave velocity structure of tidal flats, marking the first documented multichannel approach for surface wave analysis (Gabriels et al., 1987). MASW, as with other surface wave methods, involves three general steps:

1. data acquisition,
2. data processing, and
3. inversion.

Data acquisition in SWM (surface wave methods) records surface waves to study their dispersion and attenuation characteristics. Surface wave data are collected by various receivers installed on the ground. Many acquisition techniques are used in surface-wave surveying, depending on the type of application, the depth of investigation, and the acquisition scale. Of these methods, the multichannel analysis of surface waves method is one of the most common (Park et al., 1999 ; Foti, 2000). This method is typically used to develop one dimensional (1D) subsurface shear wave velocity (Vs) profiles, but in some studies the application of MASW is to detect anomaly in subsurface properties (Arslan and Cox, 2020).

In engineering and environmental near surface applications and also in conventional exploration surveys, vertical component geophones are typically used as receivers (Srinivas et al., 2014). They are usually preferred because of their low cost, robustness, and high sensitivity. Concerning signal data storage and acquisition, commercial seismographs for geophysical

prospecting are the best choices since they have high capabilities; they have been designed to be used in the field and are robust, waterproof, and dust resistant. Modern seismographs come with field computers, allowing the adjustment of acquisition parameters and preliminary data processing on the acquisition site.

Several different types of sources are generally used for active acquisitions, such as sledge hammers for generating high-frequency surface waves, heavy wave drops, seismic guns, and explosives for low-frequency waves to observe deeper parts of the subsoil. Moreover, for generating the controlled harmonic waves, other alternative continuous sources are appealable, differing by their sizes from small electromagnetic shakers to large truck-mounted vibroseis. The drawbacks of such sources are their high cost and long acquisition time (Foti et al., 2014). selecting a seismic source with the appropriate frequency bandwidth should be based on the desired testing depths, considering the relationship between penetration depth and surface wave frequency. In the example shown in Figure 4, we can see the application of Sledge hammer as a surface wave source.

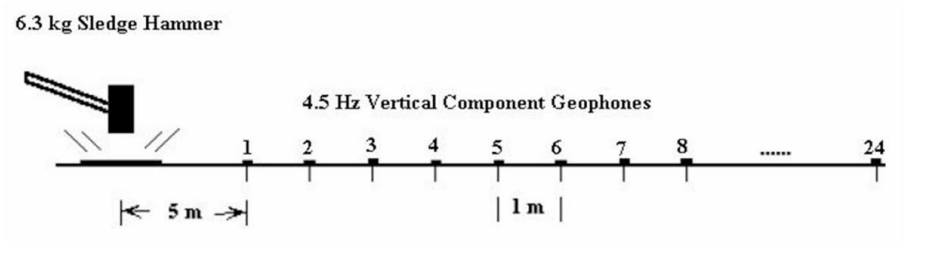

Figure 4: Channel MASW acquisition diagramme. (Srinivas et al., 2014)

In the method of MASW, surface waves are actively generated and recorded along their propagation direction on a linear array of receivers. The number of receivers in the array can vary from 12 to 96, and the spacing between them is typically between 0.5 and 5 m. The horizontal resolution of the data is influenced by the length of the receiver array, so it is important to carefully choose the testing parameters and depth range of investigation (Park, 2005). Usually, the receiver array length should be at least twice the investigation depth or equal to the maximum desired wavelength (Foti et al., 2018).

3.4. Processing and inversion

As mentioned before, one of the most common uses of the dispersive properties of surface waves is to obtain a shear wave velocity (V_S) profile by analyzing the fundamental mode of Rayleigh waves. The wave field is sampled in space and time. The acquired records are used to analyze the propagation properties for imaging or inversion processes, determining the spatial distribution of subsoil characteristics and the site's dynamic behavior (Socco and Strobbia, 2004).

Surface wave signals are grouped, and without signal processing, it is impossible to judge the quality of the signal over the desired frequency range. The first step in estimating the propagation parameters of surface waves is mainly applying the Fourier transform technique,

which transforms the data from the time domain to the frequency domain. This technique allows us to separate the frequency components of our interest for estimating the V_s using different approaches. The choice of approach depends on the number of sources and receivers and their configuration. The propagation parameters of surface waves in a media are represented as the experimental dispersion curve. Initial data in the time domain typically are transformed to the wavenumber-frequency (F-K) spectrum through the Fourier transform technique, and the peak values on F-K domain data, basically compose the dispersion curve. According to the formula below, the phase velocity of surface wave, vp, is given as a function of the wavelength λ (lambda) and time period T as:

$$v\text{p}=\lambda T$$

Equivalently, in terms of the wave angular frequency ω, which features angular change per unit of time, and wavenumber (or angular wave number) k, which is related to the angular change per unit of space,

$$v\text{p}=\omega k.$$

Phase velocity is calculated after k, and we can produce phase velocity vs frequency diagrams, allowing us to pick the high-energy frequencies of the surface waves, called the fundamental mode.
In Figure 5, a schematic view of the two main strategies for solving the problem of wave propagation parameters is shown. The result of the forward model is the basis of any inversion strategy which results in the final goal, the velocity model of the Rayleigh wave in the area of study.

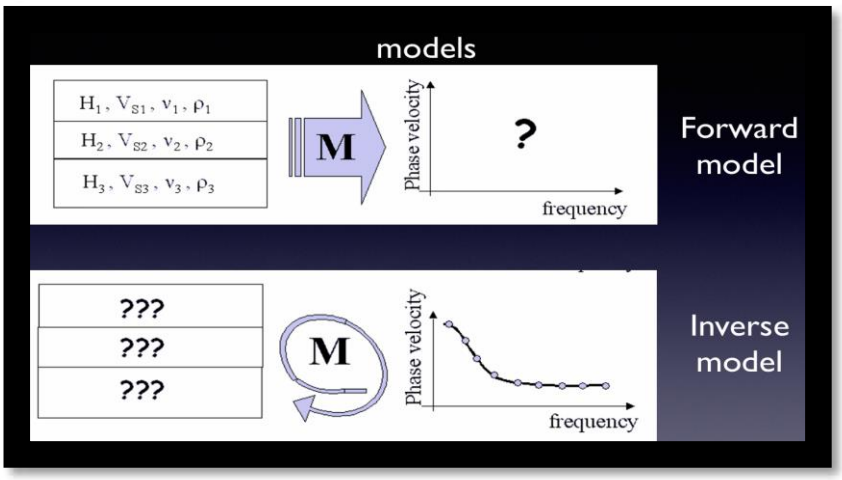

Figure 5: Problem solving strategies. (from environmental and engineering geophysics course material, department of geoscience, UNIPD)

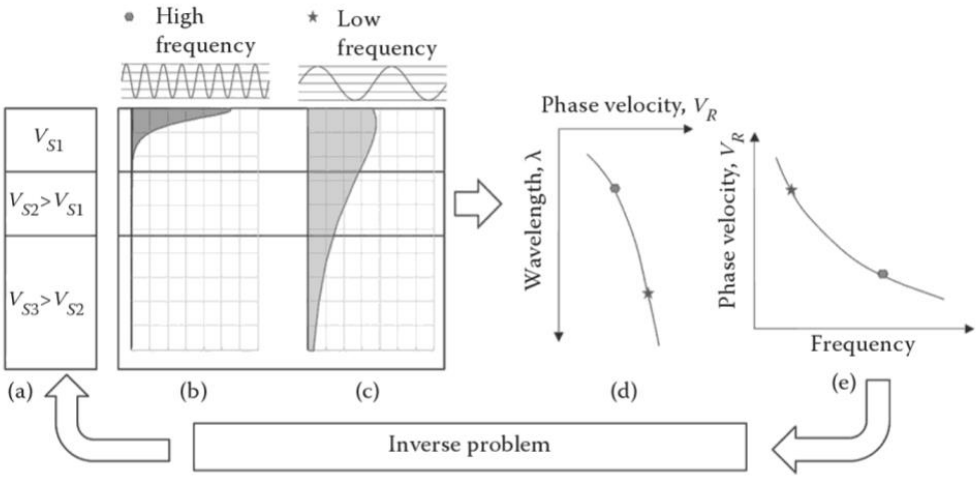

Figure 6: inversion procedure. (Foti et al., 2014)

In the forward modeling, a set of model parameters for the soil deposit is assumed and the result is a theoretical dispersion curve. Surface wave propagation and soil parameters, which are represented in the form of a dispersion curve, typically are estimated according to the initial information about the field, such as previous geological surveys' results or drilling investigations (Foti et al., 2014). Figure 6 shows schematically the inversion procedure.

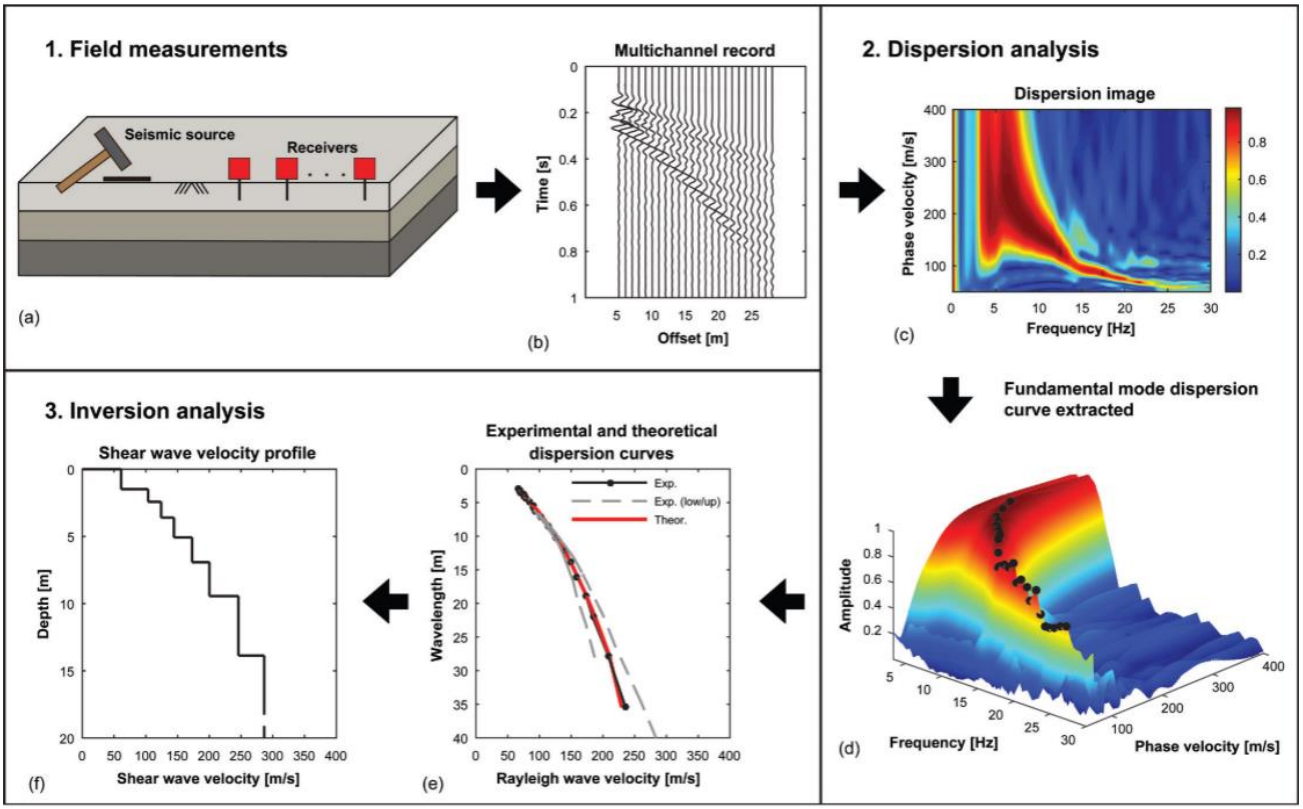

Figure 7: Overview of the MASW method: (a, b) field measurements; (c, d) dispersion analysis; (e, f) inversion analysis. (Olafsdottir et al., 2018)

As a summary, the example shown in Figure 7, represents a brief view of the MASW procedure including field measurements, dispersion analysis and inversion analysis. The initial data collected from the field, that is in time domain are transformed to frequency domain and displayed in a F-K diagram, the phase velocity vs frequency diagram. In this F-K diagram the highest amplitudes are picked to estimate the dispersion curve. The final velocity profile is generated based on the picked dispersion curve. It is good to mention that for a case of study one unique velocity profile does not exist. Inverse problems are ill-posed, and the best results would be the velocity profiles that the theoretical dispersion curves associated with them, have the least difference in comparison with the experimental dispersion curve.

3.5. Ambient noise and horizontal -to- vertical spectral ratio analysis

Ambient vibrations, also known as ambient noise or microtremors, are small ground movements that occur constantly due to natural and human-made sources. Unlike major seismic events such as earthquakes, ambient noises are continuous, low-energy vibrations that do not cause noticeable shaking but can be identified by sensitive seismometers. They provide valuable information about subsurface conditions and the dynamic properties of the ground. Their continuous nature and low amplitude make them a useful tool for non-invasive geophysical investigations and for improving our understanding of site-specific seismic hazards. The ambient seismic wave field is excited by oceanic gravity waves primarily. This can be categorized as the Earth's background free oscillations or seismic hum (1–20 mHz), primary microseisms (0.02–0.1 Hz), and secondary microseisms (0.1–1 Hz). This noise is not specific to any instrument or location, but rather is widespread and can be recorded anywhere. Figure 8 shows a typical power spectrum of the ambient seismic wave. The vertical axis shows power spectral densities of ground acceleration. The ambient seismic wave field frequency ranges from 1mHz to 100 Hz. Below 1 Hz, the dominant source of this wave field is oceanic gravity waves (specifically, ocean swell, wind waves, and ocean infragravity waves[2]) (Nishida, 2017).

[2] Ocean infragravity waves: They are long-period waves that exist within the frequency range below the traditional wind-generated ocean waves and above the tidal frequencies.

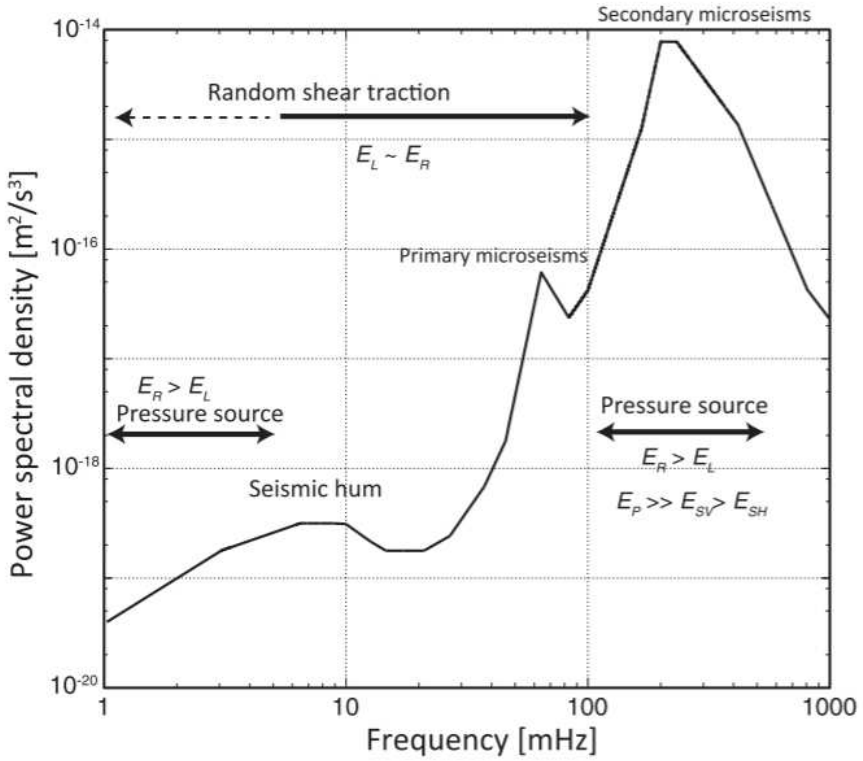

Figure 8: Typical power spectrum of the ambient seismic wave. Here, EL is the energy of Love waves, ER is that of Rayleigh waves, EP is that of P waves, ESV is that of SV waves, and ESH is that of SH waves (Nashida, 2017).

Microtremor is a very convenient tool to estimate the effect of surface geology on seismic motion, that is the term response spectrum, without needing other geological information (Nishida, 2017). To determine the response spectrum for a site (Nakamura, 1989) offers an inexpensive and easy-to-use method. It analyzes ambient seismic noise, which is always present in the shallow layers of the earth. The technique consists in estimating the ratio between the Fourier amplitude spectra of the horizontal (H) to vertical (V) components of ambient noise vibrations recorded at one single station. "The horizontal-to-vertical spectral ratio (HVSR)" is commonly used to estimate a site's resonance frequency (f_0) or the predominant frequency of the soil based on ambient noise measurements. This is the frequency at which the greatest increase of this ratio occurs due to conditions below the recording point. For sites with a strong impedance contrast, the HVSR peak frequency ($f_{0,HVSR}$) is considered a good estimate of f_0. However, the random nature of ambient noise, along with variable environmental conditions and sensor coupling issues, can lead to uncertainty in $f_{0,HVSR}$ estimates. (Nakamura, 1989) This method of seismic investigation first proposed by Nogoshi and Igarashi, (1971) and Nakamura (1989), HVSR gained popularity because it is a fast, convenient and noninvasive method which is simple in sense of field acquisition and signal processing. One theory developed by Nakamura hypothesizes that the HVSR represents the SH-wave[3] transfer function, wherein the horizontal particle motions are amplified at the resonant frequency in comparison to the vertical particle motion. According to this theory, the HVSR peak frequency is assumed equal to the site's resonance frequency, although we should always

[3] SH-wave: vertically propagating, horizontally polarized shear wave.

keep in mind that the results of this method should be expressed statistically and should not be used directly. Nakamura also suggested HVSR amplitudes to be used to infer the site amplification factor. However, most research studies show that the HVSR amplitudes should not be used to directly infer amplification factor due to the weak correlation between that and the actual site amplification (Cox et al., 2021a). However, there is a general trend for the H/V peak amplitude to underestimate the actual site amplification. In other words, the H/V peak amplitude could generally be considered as a lower bound of the actual site amplification (Teves Costa, 2004).

Another theory is that the ambient noise consists of surface waves, but several researchers have shown that the relative contribution of different waves may vary significantly from site to site as the impedance ratio changes (Cox et al., 2021). (Bonnefoy-Claudet et al., 2008) estimated the contribution of different seismic waves (body/surface waves, Rayleigh/Love waves) at the H/V peak frequency and shows that the common assumption that almost all the ambient noise energy would be carried by fundamental-mode Rayleigh waves is not justified. The relative proportion of wave types depends on site conditions, especially impedance contrast. For the 1D horizontally layered structures presented in (Bonnefoy-Claudet et al., 2008) the H/V peak frequency always provides a good estimate of the fundamental resonance frequency, whatever the H/V peak origin (Rayleigh wave ellipticity, Airy phase of Love waves, *S*-wave resonance). Moreover, it is also inferred that the relative proportion of Love waves in ambient noise controls the amplitude of the H/V peak.

Obtaining the f_0 points to the fact that microtremors can be used for microzonation studies (Lachet et al.,1996). Microzonation is a detailed analysis and mapping process that identifies variations in seismic hazard and risk within a localized area, such as a city or town. It involves dividing the area into smaller zones, each characterized by its specific seismic response, soil conditions, geological features, and potential for earthquake-induced hazards like liquefaction, landslides, and ground shaking intensity. The goal is to provide detailed information to guide urban planning, building codes, and disaster preparedness strategies. Moreover, knowledge of the resonance frequency of the soil could be used to predict the kinds of buildings that are likely to suffer the greatest damage. This method seems very suitable for site effect evaluation in urban areas since it requires only noise recorded by one three-component station (Lachet et al., 1996).

The diagram in Figure 9 visually represents the standard process used to analyze HVSR data from ambient noise recordings. The noise records, which include north-south (NS), east-west (EW), and vertical (V) components, are typically divided into multiple time windows. These windows should be 10 times longer than the estimated fundamental site period(Teves Costa, 2004). Although the example illustrates only four-time windows for simplicity, it is common to use more. HVSR curves are calculated by comparing the Fourier amplitude spectra of the horizontal and vertical components from each time window. While each horizontal component (EW and NS) can be analyzed separately, the most common approach is to combine the two horizontal components. Various methods exist to combine the horizontal components not covered in this thesis (Cox et al., 2021). However, the two most popular approaches are based on calculating the geometric mean or the quadratic mean/squared average (Cox et al., 2021).

The frequently used squared average is available in the popular open-source software package Geopsy. In the deterministic method, the peak frequency of the median HVSR curve ($f_{0,mc}$) is typically chosen as a single value of the site resonance frequency. In the probabilistic method, a sample set of f_0 values results from collecting separate f_0 values for each time window; these samples are denoted as $f_{0,i}$, where i indicates the ith window. Statistics such as the mean (μf_0) and standard deviation (σf_0) of f_0 can then be computed from the sample set. It is common that $f_{0,mc}$ is not equal to μf_0, as illustrated in Figure 9.

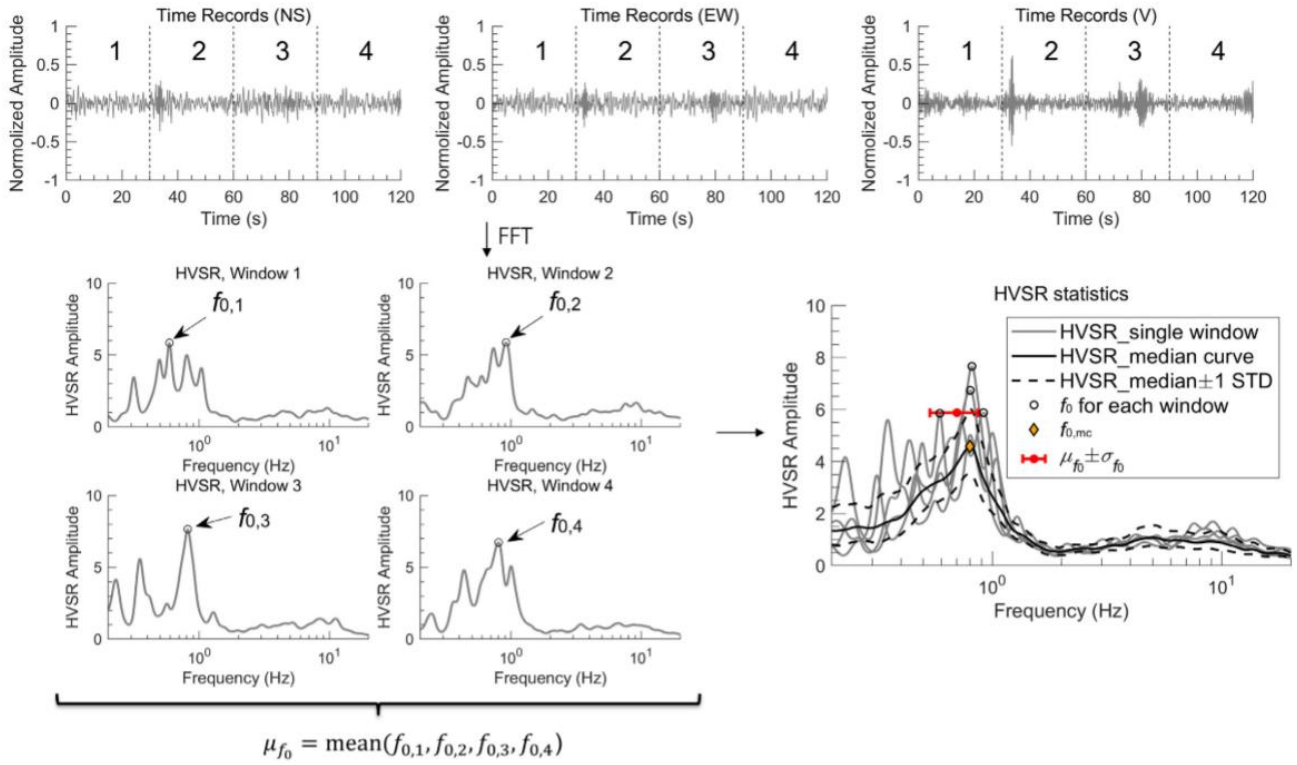

Figure 9: Schematic illustrating the common procedure used to obtain a median HVSR curve and the peak frequency of the median curve (f0,mc) from several ambient noise time windows. Also shown are the f0 values for each individual HVSR curve (f0,1, f0,2, f0,3, f0,4) and the statistics (mean, μ f0, and standard deviation, σf0) computed from the sample set (*Cox et al., 2021).*

4. Software and tools

This chapter describes the software and tools used for the data collections and analysis in "Porto tolle" project. The details of their applications in this project are discussed in detail in the methodology chapter.

4.1. Geopsy and Dinver

Geopsy, an open-source software package, helps analyze geophysical data in the seismic and geotechnical fields. Geopsy originated as part of the SESAME European Project; it offers resources for analyzing ambient vibrations with a focus on site characterization. Over time, it has integrated more traditional methods like MASW or refraction to provide a thorough, high-quality, and cost-free system for interpreting geophysical studies. It was released in 2005 as a significant outcome of the SESAME project and was developed by the highly skilled SESAME team (Wathelet et al., 2020).

In case of passive ambient noise analysis using horizontal -to- vertical spectral ratio method, Geopsy has been recognized as a reference tool for analyzing ambient vibration data in the context of site characterization studies. The versatility of geopsy allows for the processing of all kinds of data needed in site characterization studies, from single station single trace to three-component array recordings. This tool extracts Horizontal to Vertical (H/V) spectral ratios from various types of vibration signals, including ambient vibrations and earthquakes.

Dinver software is an inversion application that functions to get density, V_p, V_s, and depth. The density, V_p, V_s, and depth values can be calculated via Ms. Excel to obtain other parameters (Yulianto and Yuliyanto, 2023). This software is in the same package as the geopsy software and implements forward computations for surface waves and refraction analysis. It handles phase and/or group dispersion curves for Rayleigh and/or Love waves. Additionally, it computes refraction travel times for V_p and/or V_s (Geopsy.org).

4.2. Data Collection Tools

As mentioned, this project involved active and passive seismic data acquisition. In the case of active acquisitions, the receivers we used were vertical “Geophones”. A geophone is a device that detects acoustic vibrations within the Earth. Geophones have traditionally been passive analog tools consisting of a spring-mounted wire coil that moves within the magnetic field of a case-mounted permanent magnet to produce an electrical signal. Modern designs utilize microelectromechanical systems (MEMS) technology, which uses an active feedback rotation to create an electrical response to ground motion (Reynolds, 2011). Although waves passing through the Earth have a three-dimensional nature, geophones are normally constrained to respond to single dimension - usually the vertical. Some applications require the use of the full wave, and for this, three-component or 3-C geophones are used. In Figure 10, typical 1C geophones are shown. In this project we used geophones with a natural frequency of 4.5 Hz (i.e. the lowest frequency among those in common use, in order to guarantee the greatest possible penetration depth).

The ground roll or surface waves also produce vertical motion that may overshadow the weaker vertical signals. Using big arrays set to the same wavelength as ground-roll can reduce strong noise signals and boost weaker data signals. Analog geophones are very sensitive

devices that can respond to very distant tremors. In Figure 11, you can see one of the active acquisition lines in the Porto Tolle project as an example of geophones array.

The sources of the active acquisitions we used in Porto Tolle are a sledge hammer and a 20 Kg weight drop as shown respectively in the pictures of Figure 11 and Figure 12. A sledgehammer is a tool with a large, flat, often metal head attached to a long handle. The long handle combined with a heavy head allows the sledgehammer to gather momentum during a swing and apply a large force compared to hammers designed to drive nails. Along with the mallet, it shares the ability to distribute force over a wide area. This is in contrast to other types of hammers, which concentrate force in a relatively small area (Vila, Bob. "Types of Hammers"). When conducting active seismic acquisition, the choice of source significantly impacts data quality.

The sledgehammer is portable, easy to use, and cost-effective, making it ideal for rapid, shallow surveys. It generates high-frequency waves suitable for high-resolution investigations. However, its energy output is limited, restricting its use to near-surface layers. It also requires physical effort, leading to operator fatigue, and is more susceptible to environmental noise.

The weight drop, on the other hand, provides higher energy output, allowing it to penetrate deeper layers, making it suitable for extensive surveys. Energy output can be adjusted for different survey conditions. However, weight drops are logistically challenging, expensive, and require more setup time. They also pose higher safety risks. Generally, the sledgehammer is ideal for shallow and quick surveys. The weight drop is preferable for deeper investigations requiring more energy and consistency despite its higher cost and complexity.

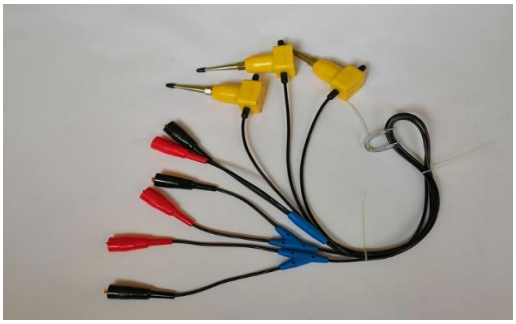

Figure 10: typical 1C geophones.

Figure 11: One of the geophone array lines in the Porto Tolle project, including the sledge hammer as the source of the MASW data acquisition.

Figure 12: The weight drop. an active seismic source in the Porto Tolle project.

In the case of passive data acquisitions, we used “Tellus-R” velocimeters or “Tritons” from the Lunitek company for the ambient noise data collection, which is shown in Figures 13 and 14. Tellus-R is a type of rotational seismometer designed to measure rotational ground motion, particularly during earthquakes. It has high sensitivity and can detect a wide range of rotational earthquake motions. One of its key features is its low noise and minimal power consumption, which makes it more advantageous. Tellus-R also includes a calibration input for periodic calibration without requiring expensive equipment. Housed in hard-coating anodized aluminum, it is well-suited for harsh environments and can operate at any orientation in space across various temperatures (Lunitek.it). Here are listed some of the main features of these velocimeters;

- Dynamic range 117Db
- Frequency range: 0.01hz ÷ 100 Hz
- Natural frequency: 1Hz/1s
- Transduction factor 50 V/rad/s
- High accuracy
- Low self-noise
- Good thermal stability
- Low power
- Robust

Figure 13: Tellus-R velocimeters from Lunitek company.

Figure 14: Lunitek velocimeter installed in the field of acquisition in Porto Tolle.

5. Location

This study was done in the “Enel power plant in Polesine Camerini” located in Porto Tolle, Rovigo, Italy (Figure 15). This site has an interesting history marked by its significant impact on the region and subsequent controversies surrounding its operations and future. The Porto Tolle Power Plant was constructed in the 1970s by ENEL (Enter Nazionale per l'Energia Elettrica), Italy's largest electricity company and located in the Po River Delta in the Veneto region.

The plant was designed to use oil as its primary fuel source. Still, in the 1980s, it was converted to burn coal, which led to significant increases in its production capacity but also brought about environmental concerns. At its peak, the plant had a generating capacity of around 2,640 megawatts, making it one of Italy’s largest power stations. The coal conversion made the Power Plant a major source of air pollution, emitting considerable amounts of sulfur dioxide, nitrogen oxides, and particulate matter. Its location in the ecologically sensitive Po River Delta, a UNESCO World Heritage site, amplified concerns about its environmental impact.

The Porto Tolle Power Plant was officially decommissioned in 2015 as part of Italy’s broader efforts to reduce reliance on coal and transition to more sustainable energy sources. Following its closure, several proposals were made to redevelop the site. Ideas included transforming it into a hub for renewable energy or a site for tourism and cultural activities. ENEL explored various options, including converting the area into a biomass power plant or a mixed-use development focusing on environmental sustainability (Enel, 2019).

Figure 15: Enel power plant in Polesine Camerini” located in Porto Tolle, Rovigo, Italy.

6. Methodology

In this study on the Porto Tolle project, we go through two acquisitions: **A**ctive seismic acquisition of multi-channel analysis of surface waves and **P**assive ambient noise characterization. Figure 17 shows a map of the area, including the locations of the data acquisition lines and sensors.

Figure 16: Location of the ex- power plant that is built on a river delta (Georicerche, 2024).

Figure 17: Detailed map of the area (QGIS software).

6.1. Data Collection

Before illustrating the data processing methodologies, we go through the data collection steps. In this project, seven lines were dedicated to active seismic acquisitions. Each line composed of 24 vertical component (1C) geophones. All lines had the same spacing of three meters between each two geophones that built 69 meters long arrays. The length of the arrays was chosen according to the desired depth of investigation which is almost 40-meter depth. The seismic source of the first two lines (L1 and L2) was a 20 kg weight drop and for the rest of the lines we used a sledge hammer to generate surface waves.

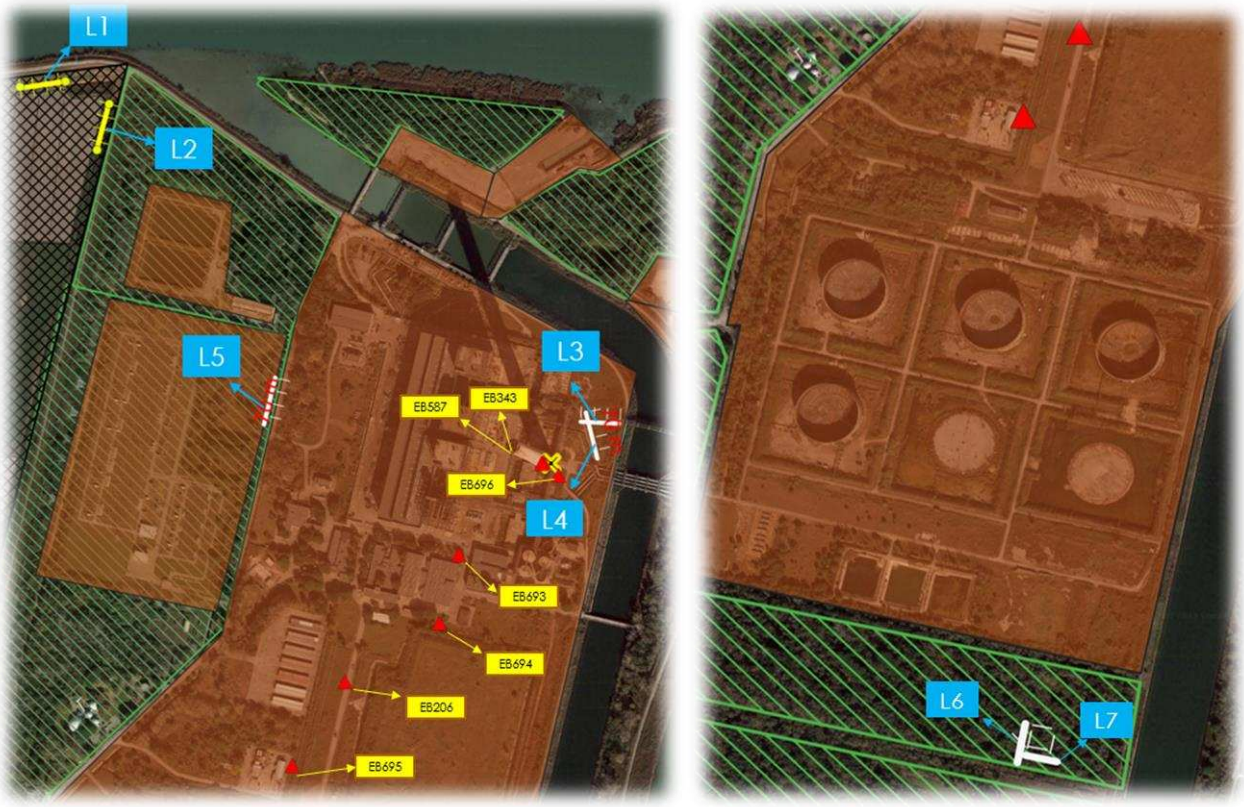

Figure 18: Location of the sensors and lines of the acquisitions (QGIS software).

When selecting suitable locations for sensors and data acquisition lines, it is important to consider the field's structural elements. As a general recommendation, it is suggested that before starting data collection, especially in the case of doing H/V measurements on the field, the team should have a look at the available geological information about the study area, in particular the types of geological formations and the possible depth to the bedrock or water tables (Teves Costa, 2004). The report of Georicerche Srl (Georicerche, 2024) accomplished on the same date as this study (01/29/2024) where the results of the geognostic investigations - 2 drillings - conducted on the same site, is a good source of geological data to obtain more initial information before doing data analyses and interpretations.

A view of Porto Tolle area is shown in Figure 16 which is built on the Po River delta in Northern Italy, so the formations of the lands in this area are young, if we don't expect to see geological complexities in this area in the first 50 m depth we expect to observe water tables in relatively low depths. We took advantage from the comparison between the results of the Georicerche Srl report and the results of this study to justify our hypothesis about the subsoil structure.

This former power plant is bordered by a water channel on the north and east sides and includes a wide concrete base covering the entire industrial area and some of the lands in the margin. It also features several inaccessible platforms occupied with pipelines, and the main element, a 250-meter (820-foot) long chimney with a diameter of approximately 28.5 meters (93.5 feet) at its widest point, which is the base of the chimney.

As shown in Figure 18, the first two lines, L1 and L2, were located in the western field area, out of the power plant platform, as were L6 and L7, in the southern woods area. In this case, we could observe the deeper layers of the subsoil in the absence of a top-coat concrete layer on these four lines' data. L3 and L4 were located near the chimney and L5 was about 400-meter away from the chimney on the west side of the area.

Along with active acquisitions, 7 Tritons (Tellus-R seismometers) were installed as the red triangles show in Figure 18 for acquiring passive data; one velocimeter labeled EB587 and an accelerometer labeled EB 343 were deployed on the top of the chimney tower while the other 5 sensors installed on the ground to the maximum distance of 500-meter from the chimney, labeled EB696, EB693, EB206, EB695 respectively. They recorded 18-hour data which is a time period suitable and enough for ambient noise analysis. Table 2 presents a summary of all the data acquisitions acquired at the site, which is discussed in detail in continuation.

LINE	MODE	COMMENTS
L1	ACTIVE	Right to left, 24 geophones, one-directional, 3-meter spacing array,2 shots, 6m offset.
	PASSIVE	one TRITON in the middle of the line,1-hour recording.
L2	ACTIVE	Right to left, 24 geophones, one-directional, 3-meter spacing array,2 shots, 6m offset.
	PASSIVE	one TRITON in the middle of the line,1-hour
L3	ACTIVE	24 geophones, one-directional,3meters spacing array, 6shots ,2m &4m&6m offset (2shots each)
L4	ACTIVE	24 geophones, one-directional,3meters spacing array, 6shots ,2m &4m&6m offset (2shots each)
L5	ACTIVE	24 geophones, one-directional,3meters spacing array, 6shots , 4m &6m &9m offset (2shots each)
L6	ACTIVE	24 geophones, one-directional,3meters spacing array, 6shots , 4m &6m &9m offset (2shots each)
L7	ACTIVE	24 geophones, one-directional,3meters spacing array, 6shots , 4m &6m &9m offset (2shots each)
TRITONS	PASSIVE	18-hour of recording of 7sensors, 2 on the top of the tower,5 on the ground near the tower.

Table 2: Acquisitions summary.

6.2. Velocity modeling, using multichannel analysis of surface waves (MASW)

This section first covers the steps for processing MASW data using Geopsy software and the inversion using Dinver software. Then, we discuss the results obtained from each line of the data acquisitions.

Working with Geopsy gives us the possibility to see the seismic section of the MASW data as the one displayed in Figure 19, to have a quick view of the raw data, and the seismic section display comes with the Signal viewer table representing the metadata of the signals (geopsy version 3.4.2). The seismic section window also allows zooming in and out in amplitude and time domains. Normalization of the data in time domain can also be done in the same window of the seismic section. As for the other tools like H/V, the data may be pre-processed before going through the rest of the analysis. There are three ways to do this;

- The filters or remove trend functions available in the waveform toolbar
- From a graphic viewer to verify the windowing and to display the raw data
- From a table as shown in Figure 20; A Table is a Signal viewer representing the metadata of a set or a subset of signals.

Geopsy is a dedicated tool for generating dispersion curves and velocity models, providing a user-friendly toolbox of **Linear F-K for active experiments**. In the Linear F-K toolbox, the user is able to set up processing parameters and see the MASW results displayed on the Linear F-K results window. As shown in Figure 21, the processing parameters to define or manipulate in this toolbox include (Geopsy.org);

- Processing tab: This tab is used to define the time window. It allows selecting the time limits, part of the signals to be processed, and the time window length, the tapering. It also allows the definition of the processing scheme (F-K or High Resolution-F-K).
- Output tab: sets up the frequency and slowness band to be processed and the beam power normalization.
- Curves tab: used to save, remove, or load the picked dispersion curves.

As shown in Figure 22, in the result window, one plot is created for each identified shot. Three velocity-picking methods are available in the result window: Manual picking, Semi-automatic picking, and Fully automatic picking. All picked curves are available under the Curves tab in the toolbox with a curve browser.

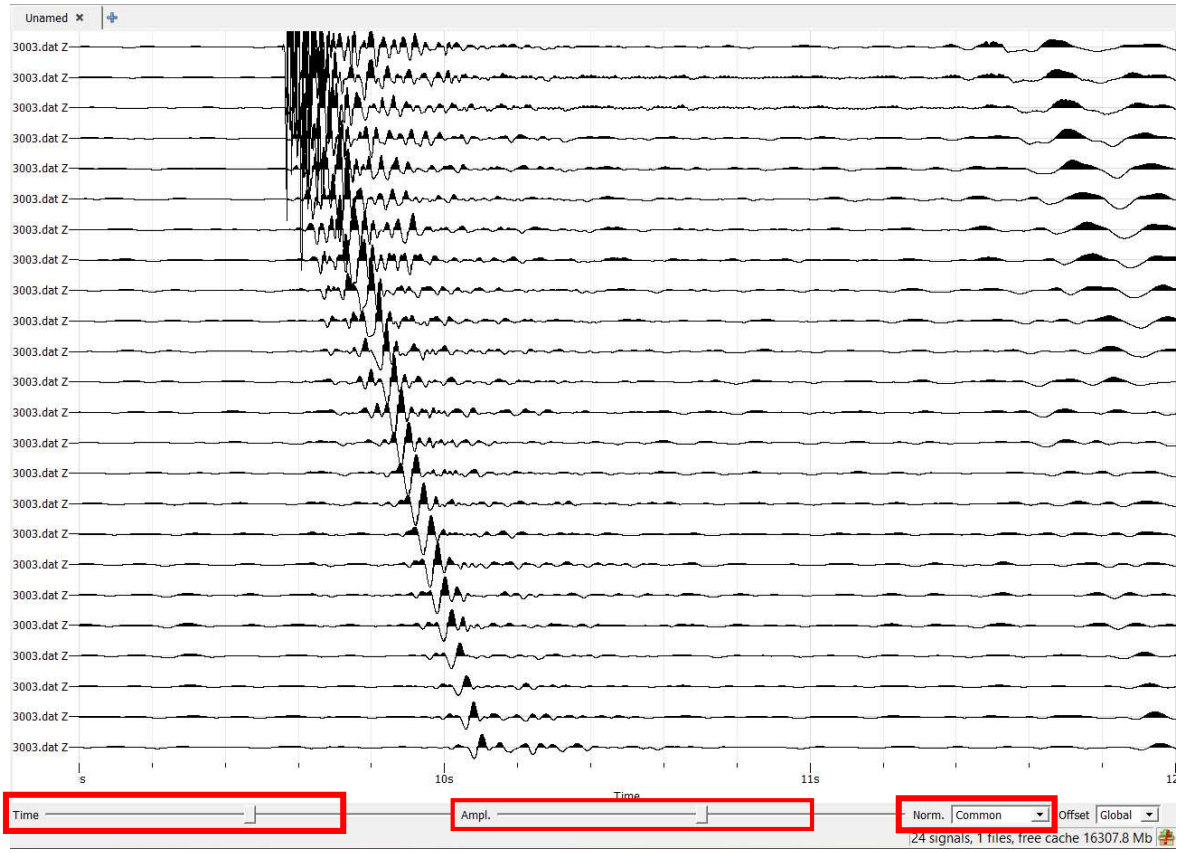

Figure 19: Example of a seismic section. The version used is 3.5.2.

	ID	Name	Component	Time reference	Start time	End time	Sampling frequency	dt	N samples	Duration	Rec x	Rec y	Rec z	Type
1	1	WA_WAU01	East	25/02/2010 00:00:00	8h19m55.000000s	8h35m34.740000s	100	0.01	93974	15m39.740000s	0	0	0	Waveform
2	2	WA_WAU01	North	25/02/2010 00:00:00	8h19m55.000000s	8h35m35.800000s	100	0.01	94080	15m40.800000s	0	0	0	Waveform
3	3	WA_WAU01	Vertical	25/02/2010 00:00:00	8h19m55.000000s	8h35m22.840000s	100	0.01	92784	15m27.840000s	0	0	0	Waveform
4	4	WA_WAU02	East	25/02/2010 00:00:00	8h19m57.000000s	8h35m39.940000s	100	0.01	94294	15m42.940000s	0	0	0	Waveform
5	5	WA_WAU02	North	25/02/2010 00:00:00	8h19m57.000000s	8h35m37.600000s	100	0.01	94060	15m40.600000s	0	0	0	Waveform
6	6	WA_WAU02	Vertical	25/02/2010 00:00:00	8h19m57.000000s	8h35m24.920000s	100	0.01	92792	15m27.920000s	0	0	0	Waveform
7	7	WA_WAU03	East	25/02/2010 00:00:00	8h20m20.000000s	8h35m57.410000s	100	0.01	93741	15m37.410000s	0	0	0	Waveform
8	8	WA_WAU03	North	25/02/2010 00:00:00	8h20m20.000000s	8h35m57.410000s	100	0.01	93741	15m37.410000s	0	0	0	Waveform
9	9	WA_WAU03	Vertical	25/02/2010 00:00:00	8h20m20.000000s	8h35m46.830000s	100	0.01	92683	15m26.830000s	0	0	0	Waveform
10	10	WA_WAU04	East	25/02/2010 00:00:00	8h20m	8h35m43.980000s	100	0.01	94398	15m43.980000s	0	0	0	Waveform
11	11	WA_WAU04	North	25/02/2010 00:00:00	8h20m	8h35m49.280000s	100	0.01	94928	15m49.280000s	0	0	0	Waveform
12	12	WA_WAU04	Vertical	25/02/2010 00:00:00	8h20m	8h35m27.520000s	100	0.01	92752	15m27.520000s	0	0	0	Waveform
13	13	WA_WAU05	East	25/02/2010 00:00:00	8h20m2.000000s	8h35m29.740000s	100	0.01	92774	15m27.740000s	0	0	0	Waveform
14	14	WA_WAU05	North	25/02/2010 00:00:00	8h20m2.000000s	8h35m31.240000s	100	0.01	92924	15m29.240000s	0	0	0	Waveform
15	15	WA_WAU05	Vertical	25/02/2010 00:00:00	8h20m2.000000s	8h35m30.280000s	100	0.01	92828	15m28.280000s	0	0	0	Waveform
16	16	WA_WAU06	East	25/02/2010 00:00:00	8h20m4.000000s	8h35m40.920000s	100	0.01	93692	15m36.920000s	0	0	0	Waveform
17	17	WA_WAU06	North	25/02/2010 00:00:00	8h20m4.000000s	8h35m36.540000s	100	0.01	93254	15m32.540000s	0	0	0	Waveform
18	18	WA_WAU06	Vertical	25/02/2010 00:00:00	8h20m4.000000s	8h35m30.970000s	100	0.01	92697	15m26.970000s	0	0	0	Waveform
19	19	WA_WAU07	East	25/02/2010 00:00:00	8h20m6.000000s	8h35m41.500000s	100	0.01	93550	15m35.500000s	0	0	0	Waveform
20	20	WA_WAU07	North	25/02/2010 00:00:00	8h20m6.000000s	8h35m38.210000s	100	0.01	93221	15m32.210000s	0	0	0	Waveform
21	21	WA_WAU07	Vertical	25/02/2010 00:00:00	8h20m6.000000s	8h35m32.870000s	100	0.01	92687	15m26.870000s	0	0	0	Waveform
22	22	WA_WAU08	East	25/02/2010 00:00:00	8h20m7.000000s	8h35m42.170000s	100	0.01	93517	15m35.170000s	0	0	0	Waveform
23	23	WA_WAU08	North	25/02/2010 00:00:00	8h20m7.000000s	8h35m41.980000s	100	0.01	93498	15m34.980000s	0	0	0	Waveform
24	24	WA_WAU08	Vertical	25/02/2010 00:00:00	8h20m7.000000s	8h35m34.640000s	100	0.01	92764	15m27.640000s	0	0	0	Waveform

Figure 20: default table view (Geopsy.org).

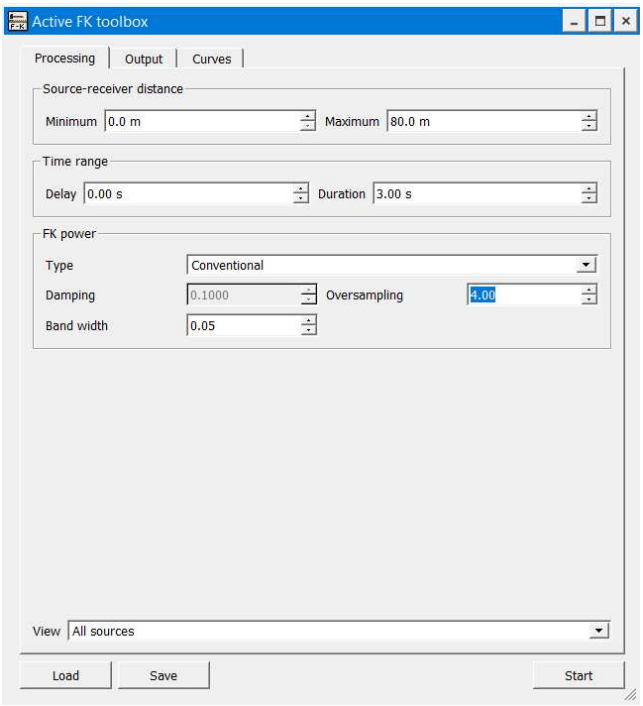

A)

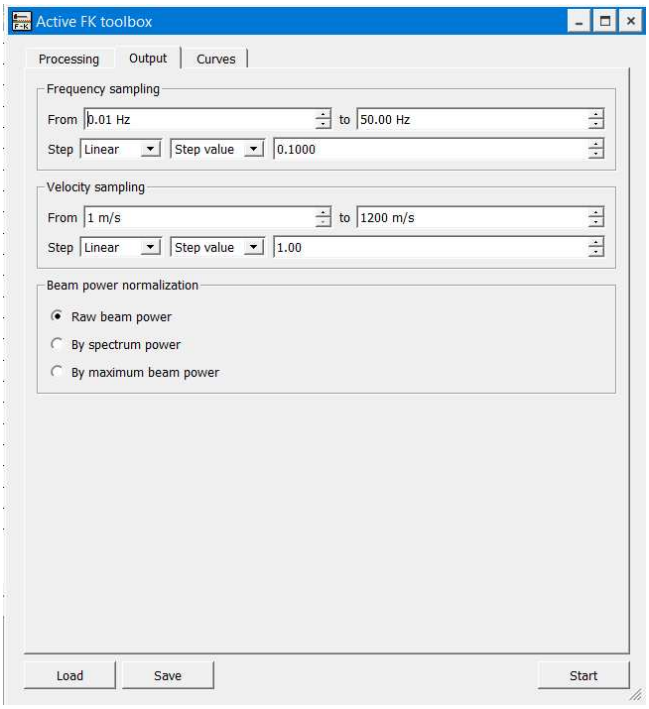

B)

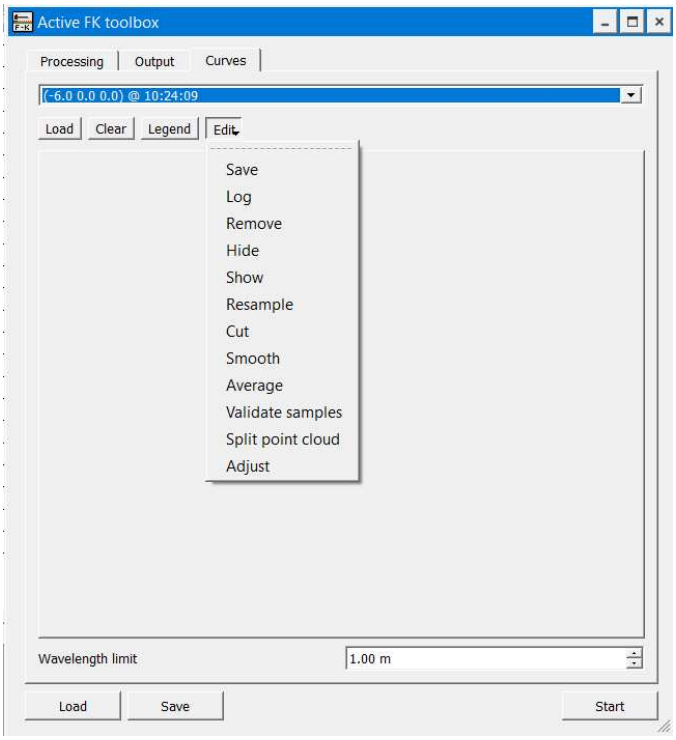

C)

Figure 21: linear active toolbox. A) processing B) output C) curves (Geopsy version 3.5.2).

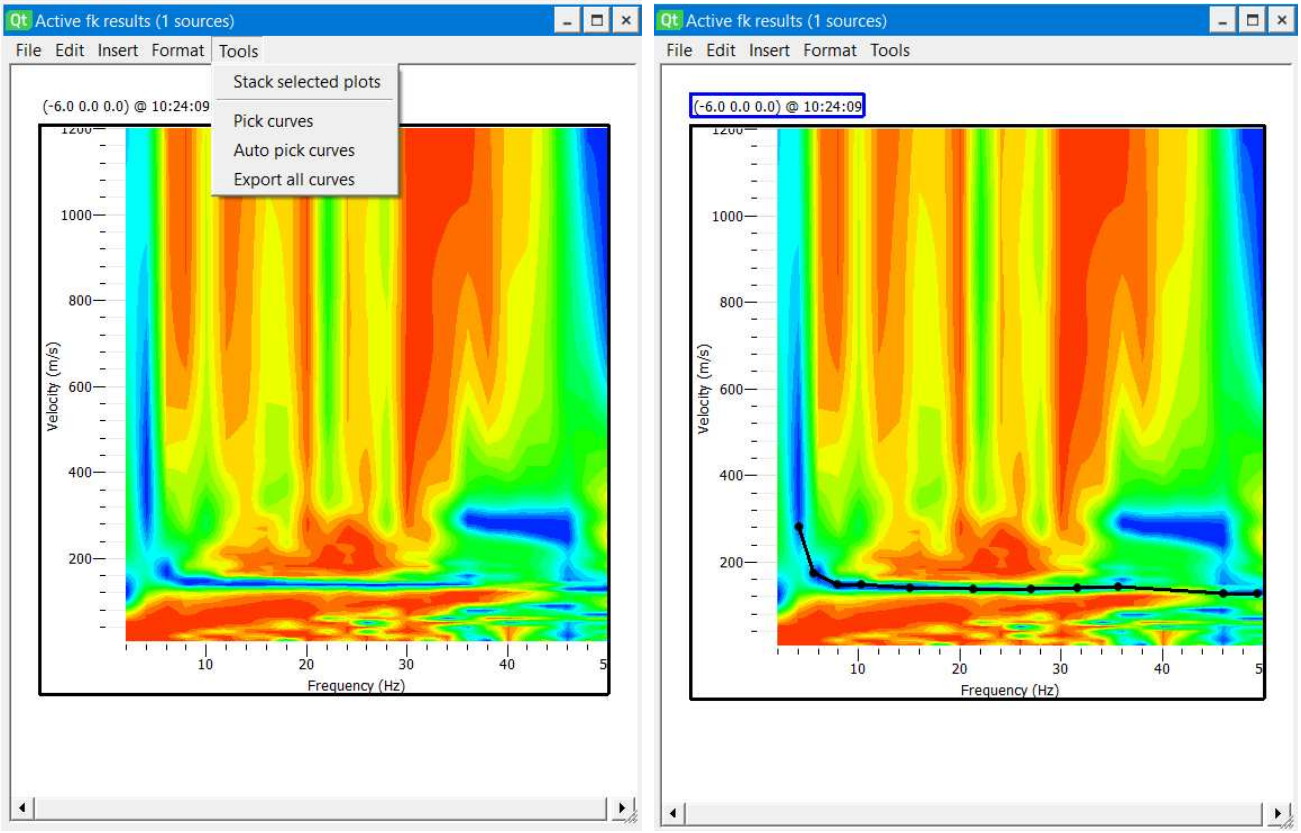

Figure 22: An example of the result window before and after the dispersion curve picking (Geopsy version 3.5.2).

There are two approaches for producing the dispersion curves: by picking the amplitudes in the frequency domain, with and without normalization of the amplitudes. Normalization of the amplitudes in the frequency domain allows us to pick even frequencies with small variations of energy amplitudes and results in more detailed dispersion curves. However, the drawback of normalization is that we consider some frequencies as parts of the fundamental mode, which might be noises. In other words, normalization highlights the noises, and the main signal would be lost or hard to see. On the other hand, the dispersion curves without normalization show us the main and principal frequency events related to the source energy with the highest amplitudes. We can identify better which main signal frequencies to pick. We can see the results of the two approaches and picked dispersion curves on the best shots on the data collected on each acquisition line in Porto Tolle in the following figures. The lines are grouped based on their location in the site, each figure belongs to one spot of the site under study. Figure 23 to Figure 26 show the dispersion curves with normalizations, while Figure 27 to Figure 30 show them without normalization of the amplitudes. As expected the frequency of the waves generated by the hammer is not below 10 Hz. The picked values below 10 Hz in the former figures, belong to the ambient noise data which are analyzed during H/V analysis on the passive data.

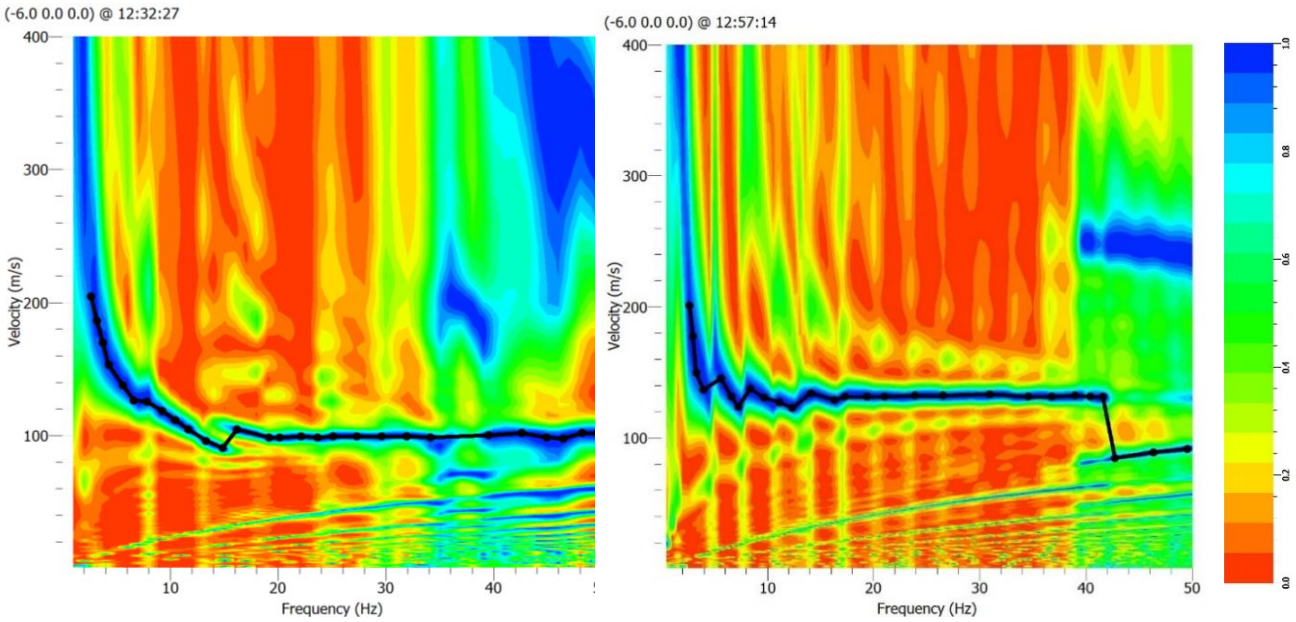

Figure 23: Dispersion curves with normalization of the amplitudes in frequency domain of the data from the lines of active seismic acquisition acquired on the west side of the site, beyond the concrete layer of the field, A) stack of 2 shots on L1, B) stack of 2 shots on L2.

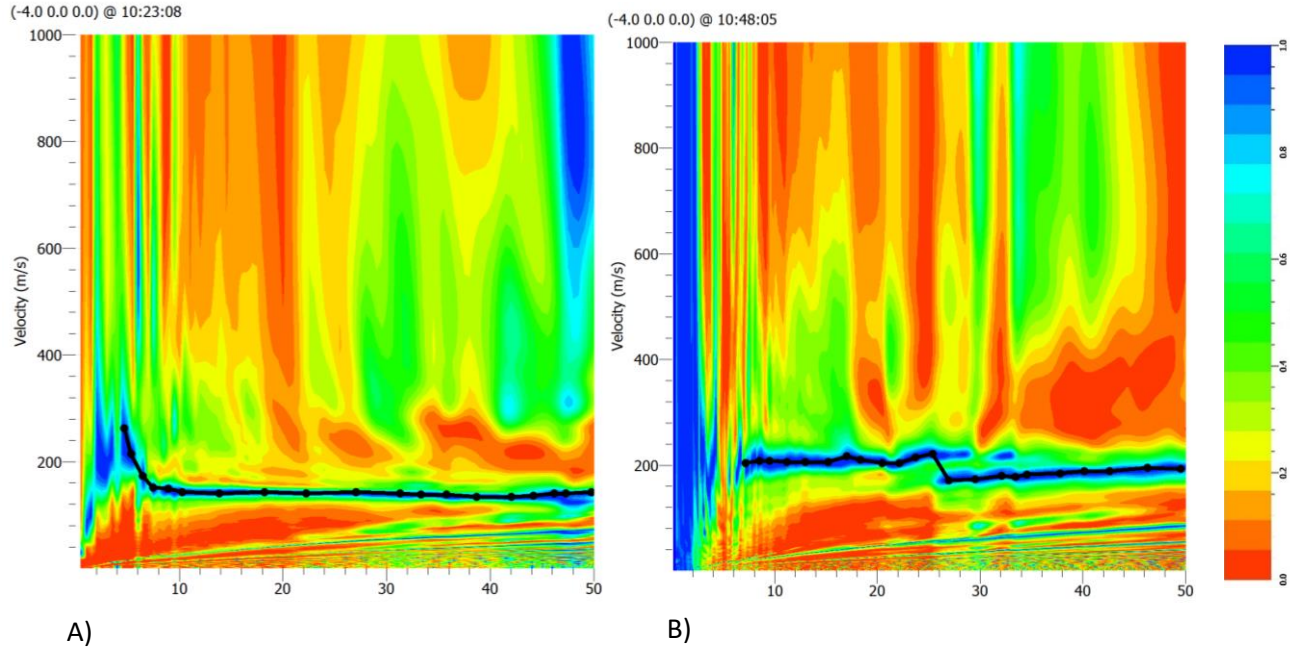

Figure 24: Dispersion curves with normalization of the amplitudes in frequency domain of the data from the lines of active seismic acquisition acquired on the closest location to the tower structure in the north east side of the site, A) shot 6 on L3, B) shot 1 on L4.

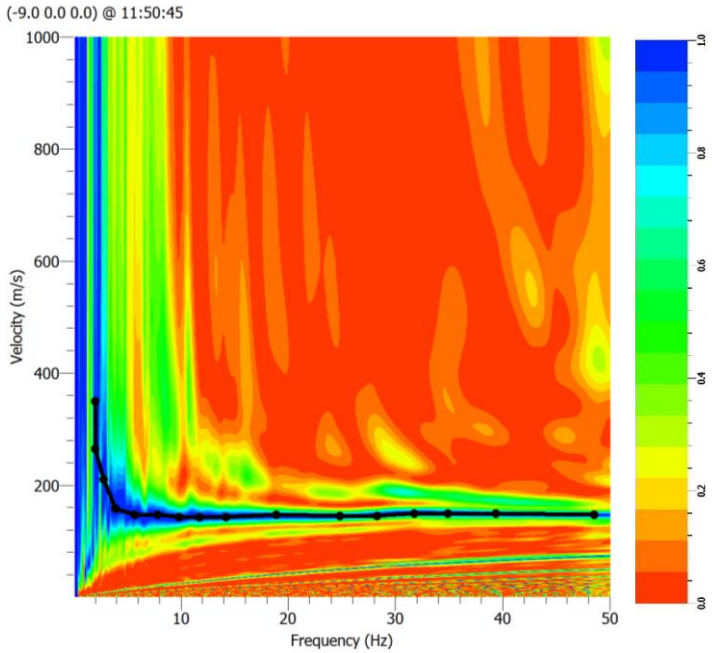

Figure 25: Dispersion curves with normalization of the amplitudes in frequency domain of the data from the lines of active seismic acquisition acquired on the west side of the site, inside the industrial part on the concrete layer, shot 9 on L5.

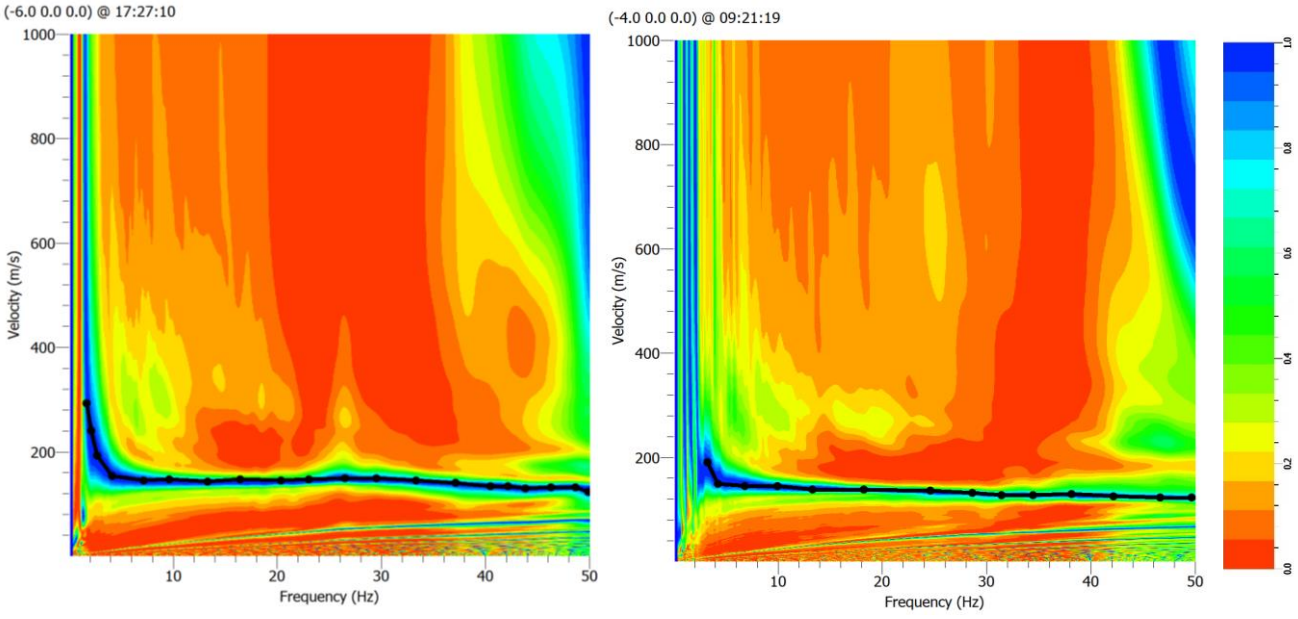

A) B)

Figure 26: Dispersion curves with normalization of the amplitudes in frequency domain of the data from the lines of active seismic acquisition acquired in the woods located in the south of the area, A) shot 3 on L6, B) Shot 3 on L7.

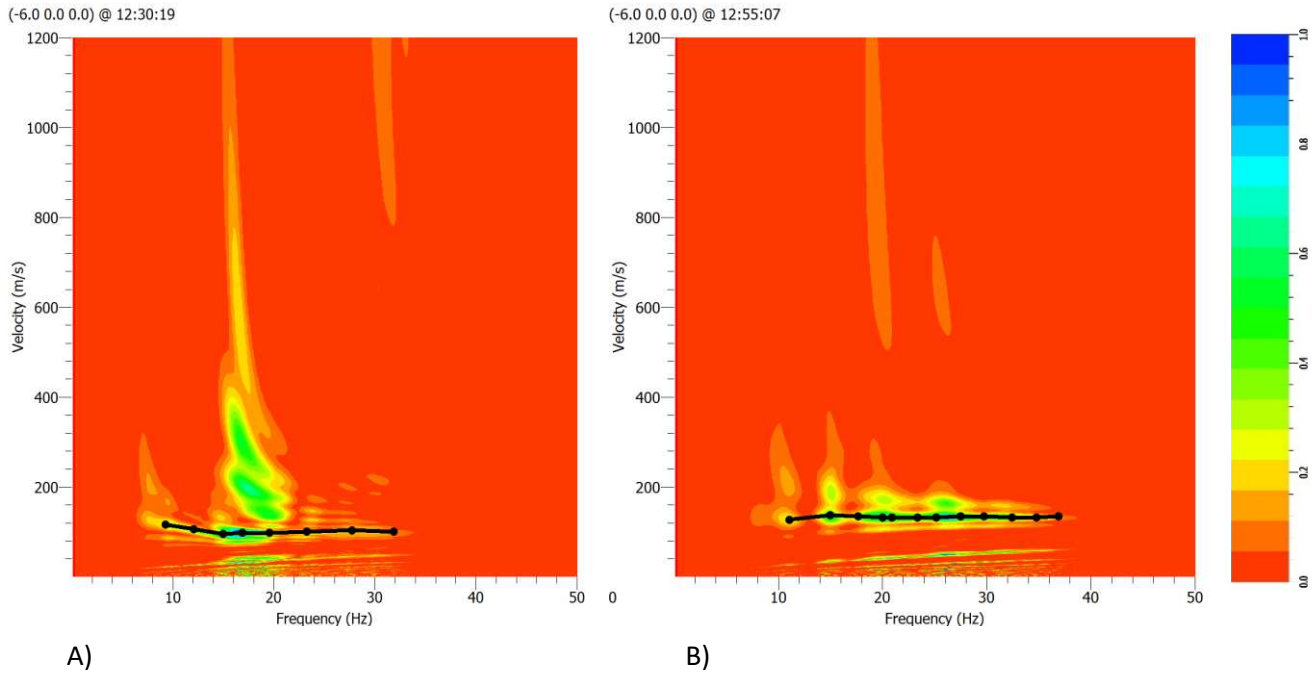

Figure 27: Dispersion curves without normalization of the amplitudes in frequency domain of the data from the lines of active seismic acquisition acquired in the west side of the site, beyond the concrete layer of the field, A) stack of 2 shots on L1, B) stack of 2 shots on L2.

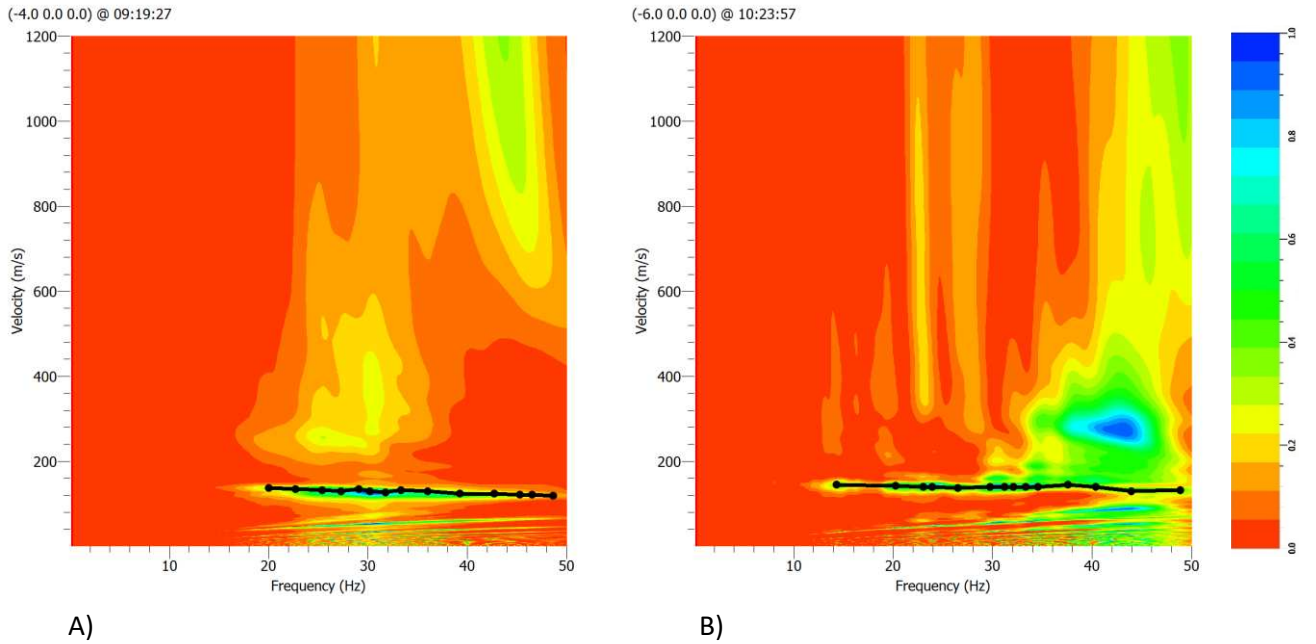

Figure 28: Dispersion curves without normalization of the amplitudes in frequency domain of the data from the lines of active seismic acquisition acquired in the closest location to the tower structure in the north east side of the site, A) shot 6 on L3, B) shot 1 on L4.

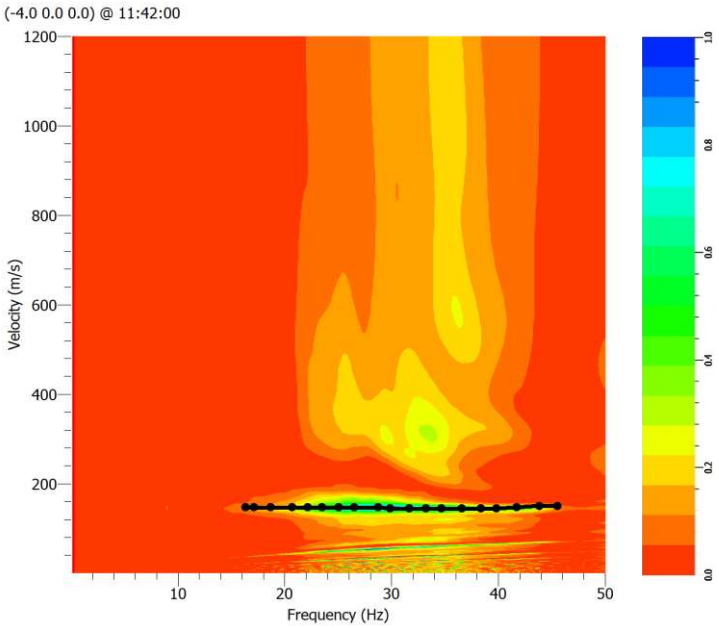

Figure 29: Dispersion curves with normalization of the amplitudes in frequency domain of the data from the lines of active seismic acquisition acquired on the west side of the site, inside the industrial part on the concrete layer, shot 9 on L5.

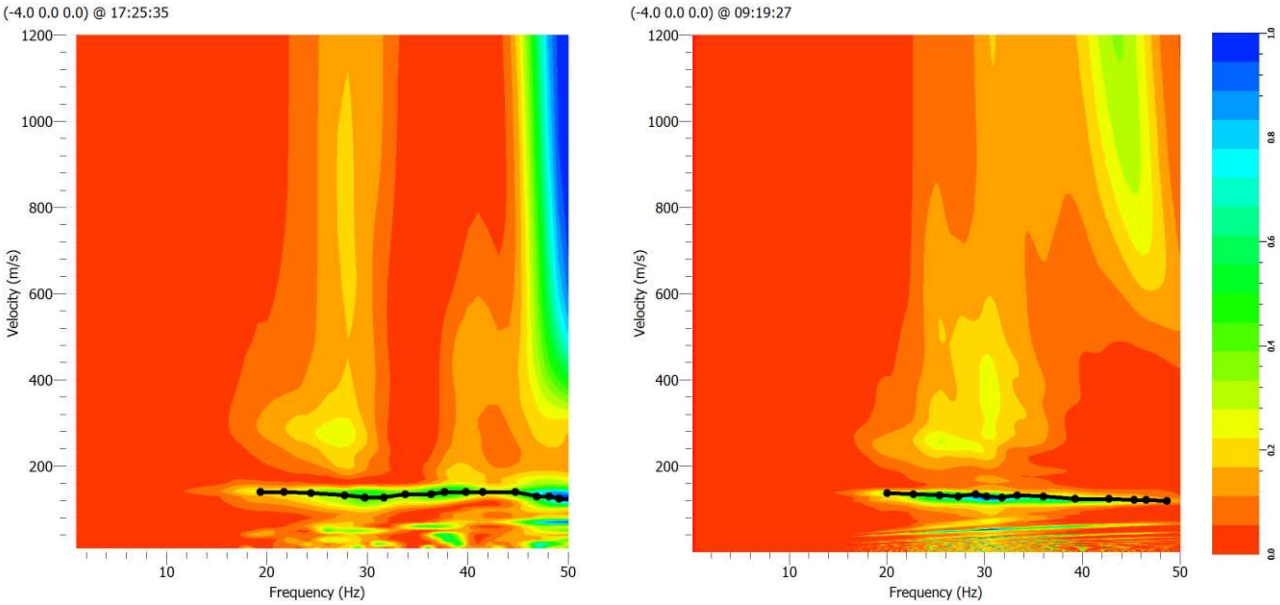

Figure 30: Dispersion curves with normalization of the amplitudes in frequency domain of the data from the lines of active seismic acquisition acquired in the woods located in the south of the area, A) shot 3 on L6, B) Shot 3 on L7.

Upon initial inspection of the dispersion curves, it is evident that the curves form relatively straight lines with small curvatures, indicating the homogeneity of the structure of the subsoil under study. This interpretation should also be supported by the velocity profiles. The inversion procedure follows the determination of the dispersion curve and allows reconstructing the vertical shear-wave velocity distribution from the observed dispersion curve (Dal Moro et al., 2007).

Inversion process starts with forward modeling. To generate a theoretical dispersion curve, a set of model parameters should be assumed for the soil deposit under study. Defining the parameter is the key point of the inversion. At this step we must figure out what information we already know about the ground structure and information we would like to extract in order to set properly the a priori information. There is no unique way of defining a correct parameterization and there is currently no commonly accepted strategy to conduct an inversion. It was a good idea to pick the first arrivals to have an initial estimation of the number of layers of the subsoil. Still, unfortunately, since the under-study lands are located on a river delta, we expect to have a water table near the surface, which does not allow us to see the first arrivals easily. In Figure 31, we look at the Stack of 2 shots on line L1. The seismic waves that pass through the water table are recorded earlier than the first arrivals, which are reflected from the interfaces of the layers. In this case we assume a one-layer structure in the first 50-meter depth. The parameter panel should look like Figure 32. The parameterization in this panel describes a ground structure with one layer with uniform V_p and V_s in the top and bottom of the layer. Computed Poisson's ratios must remain between 0.2 and 0.5 (usual values for soils and rocks).

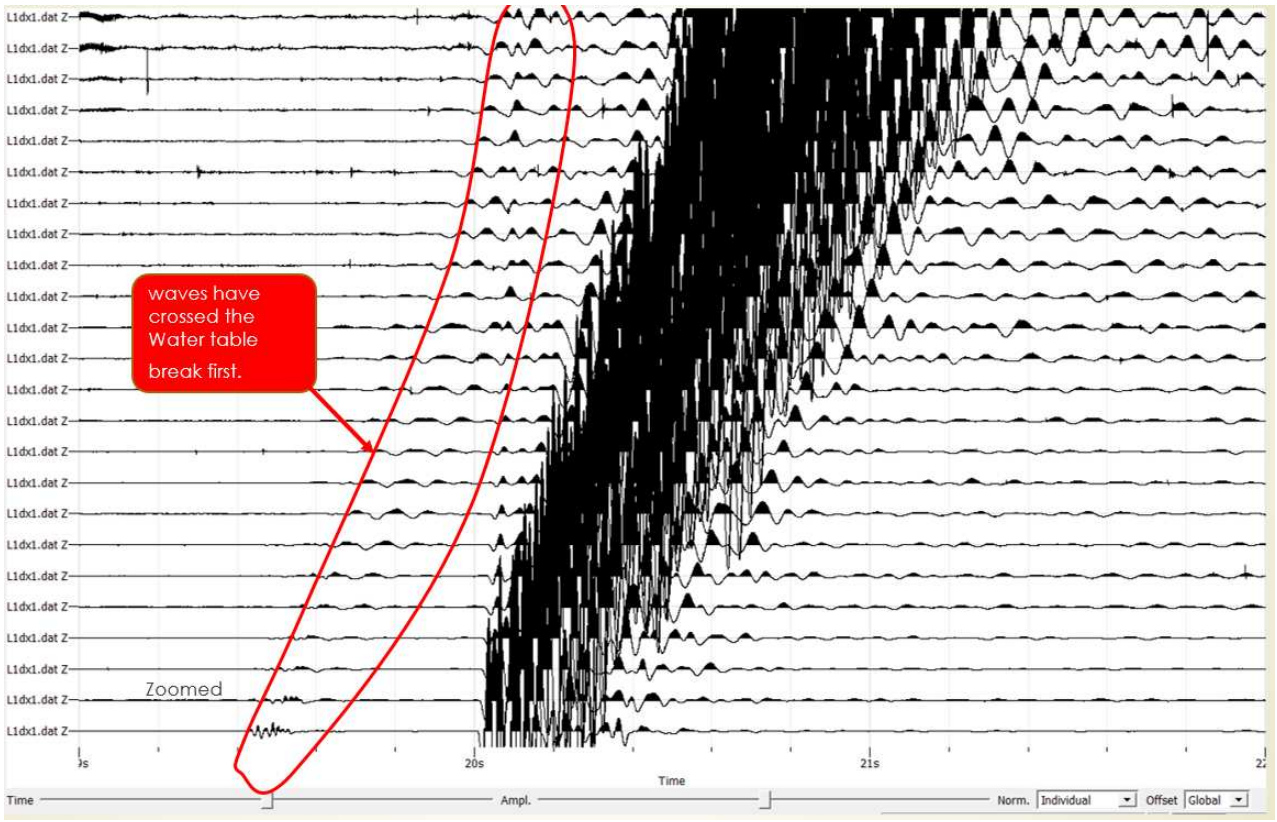

Figure 31: Stack of 2 shots on line L1.

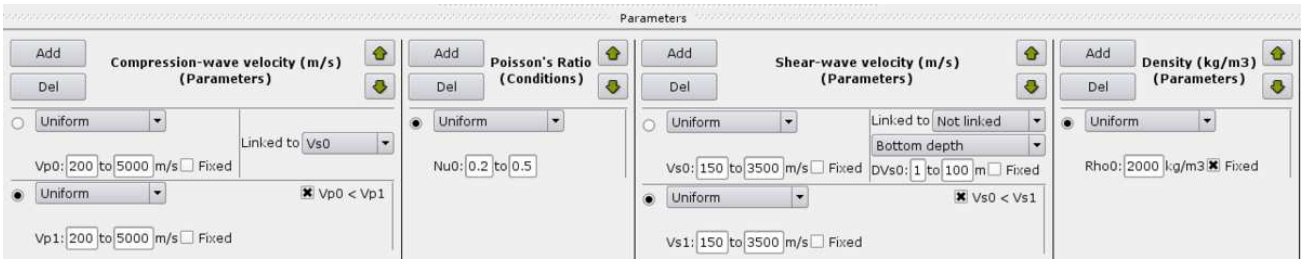

Figure 32: A 1-layer model with a uniform V_p profile and Vs in the top and bottom of the layer.

Using the technique described in Section 3.4. the experimental dispersion curves (refer to Figure 23- Figure 27) were simultaneously inverted to determine the shear wave velocity (V_S) profiles on each acquisition line. The results in Figures 33 to Figure 39, indicate that the V_S values generally exhibit minimal variation in the range of 150 to 200 m/s up to a depth of approximately 20- 25 meters across all the lines. Beyond the 25-meter depth, there is a noticeable increase in V_s values across some of the lines, e.g. line L4.

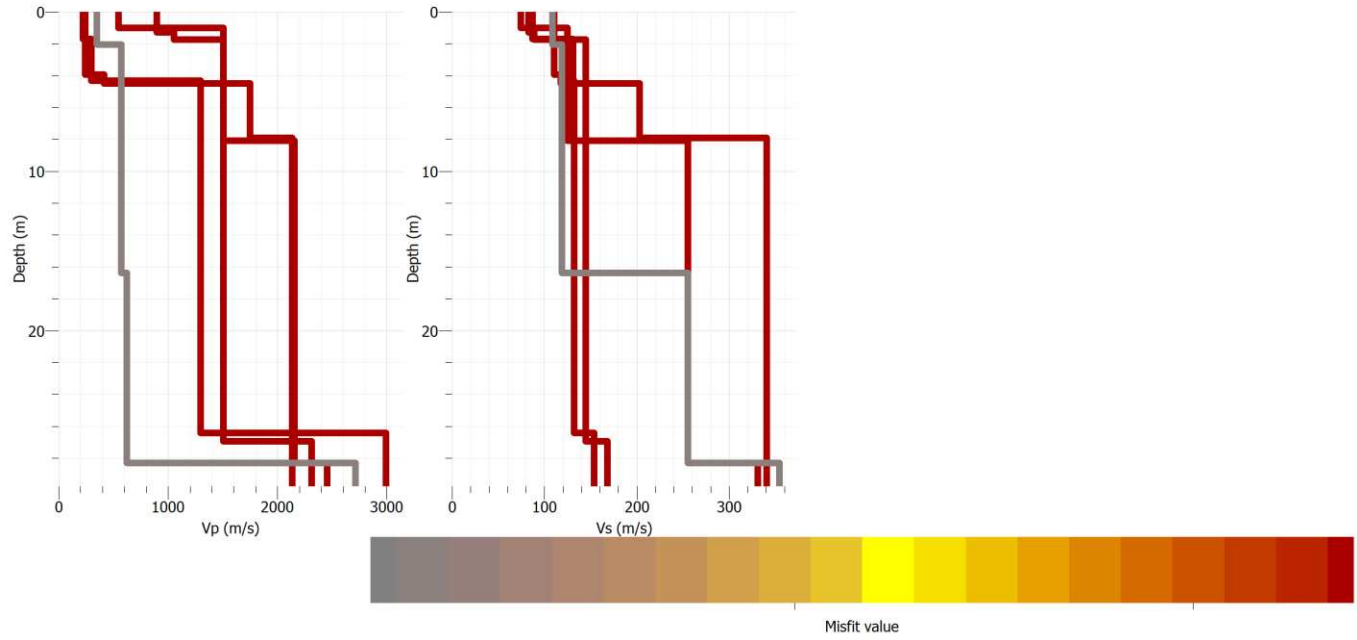

Figure 33: velocity profile of line L1.

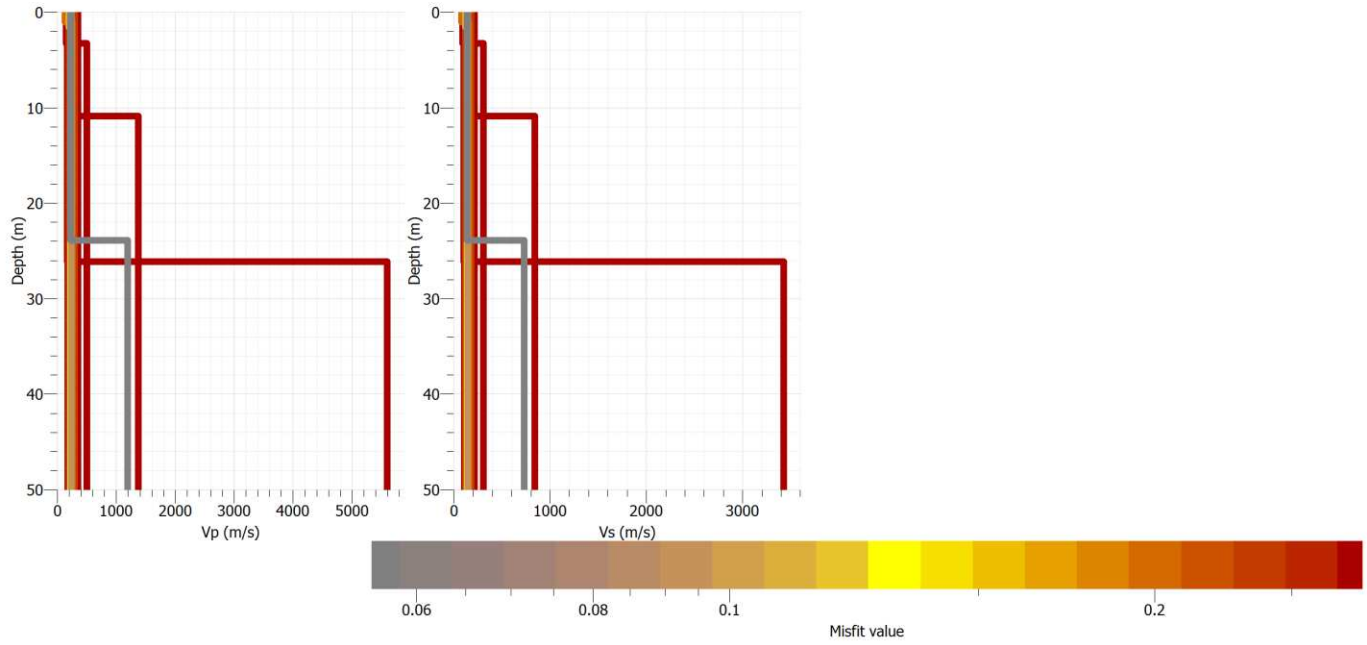

Figure 34: velocity profile of line L2.

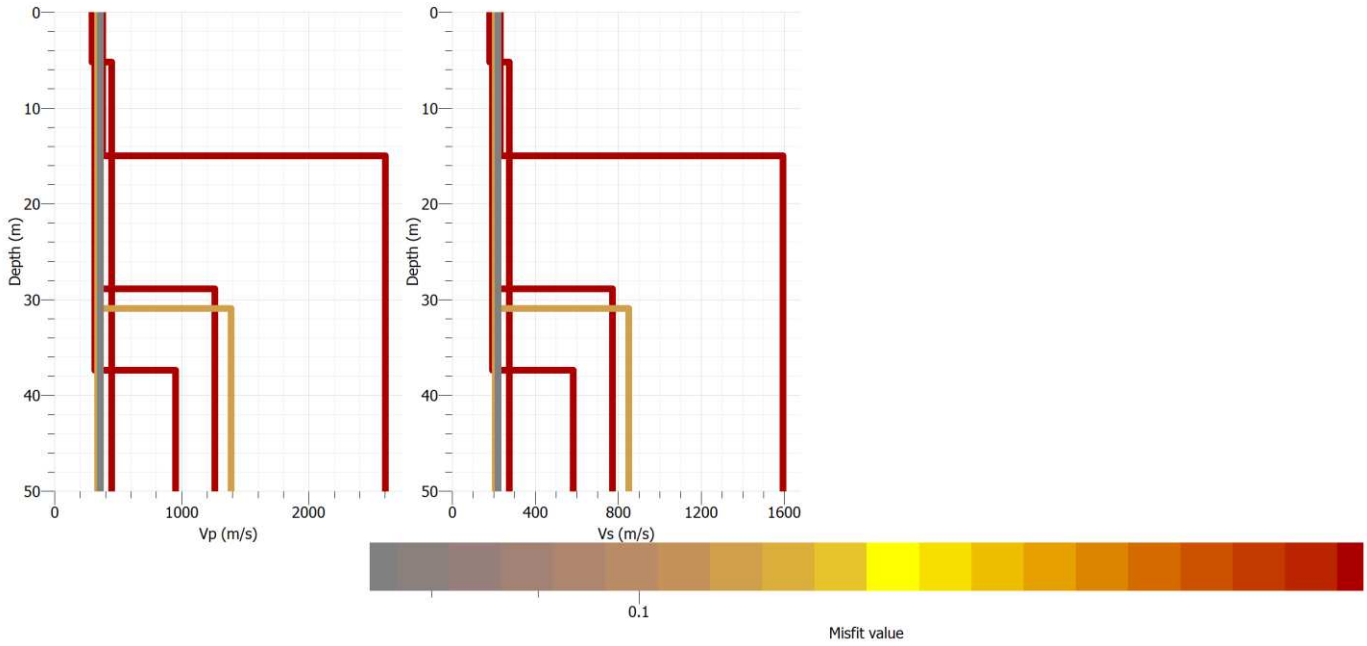

Figure 35: velocity profile of line L3.

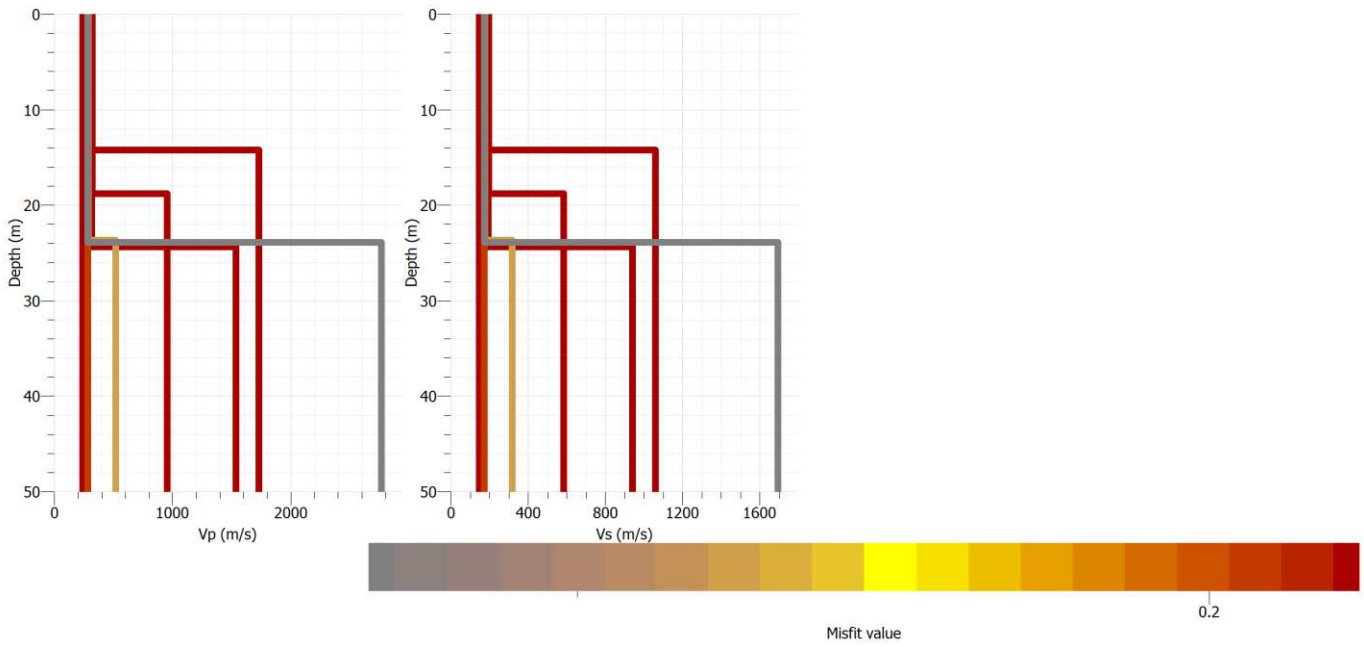

Figure36: velocity profile of line L4.

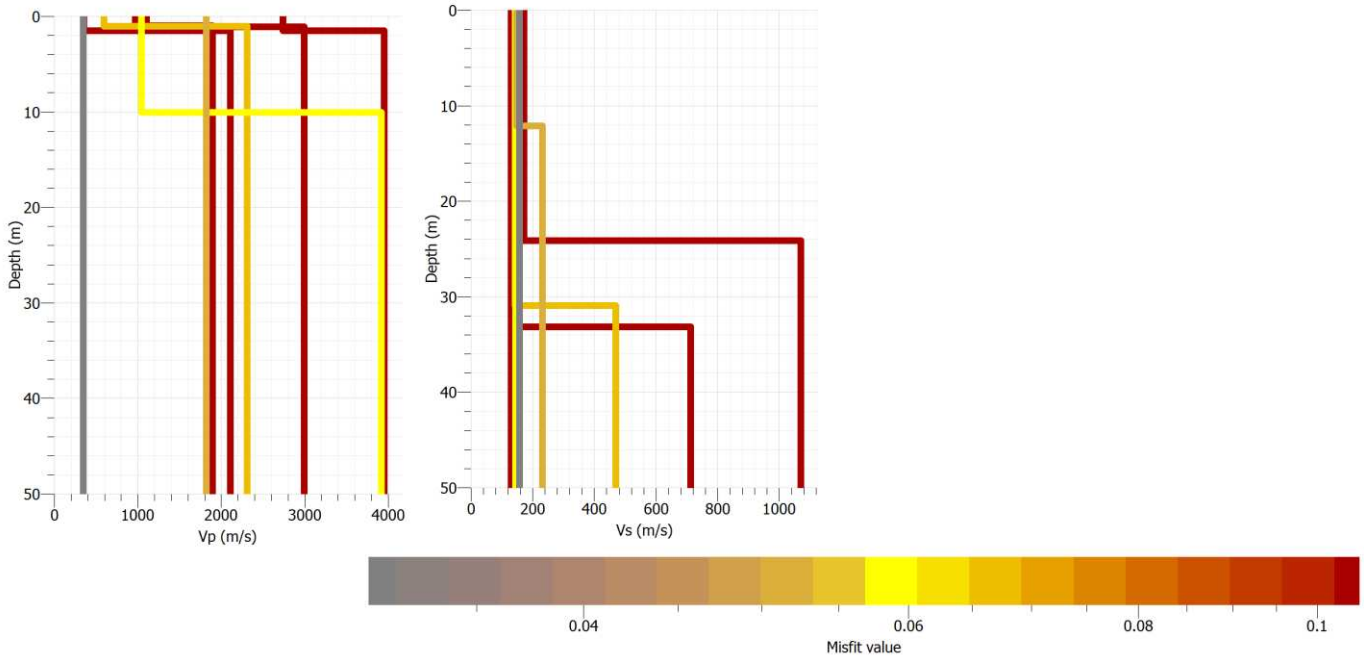

Figure37: velocity profile of line L5.

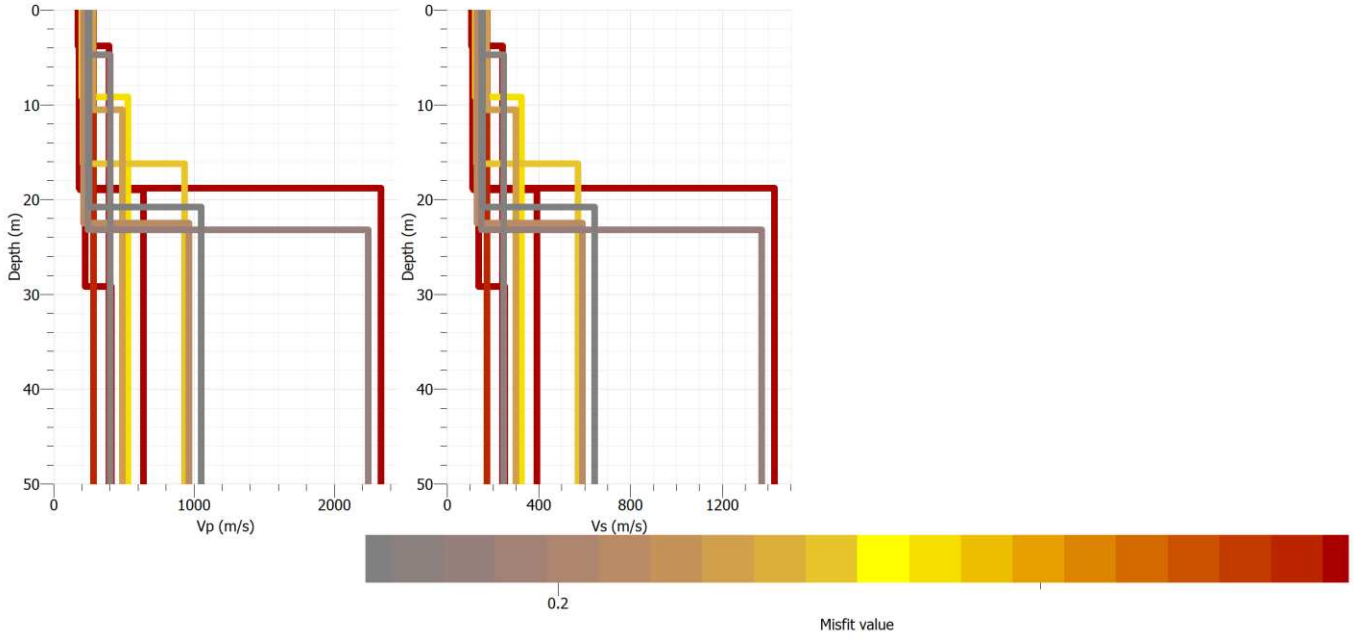

Figure 38: velocity profile of line L6.

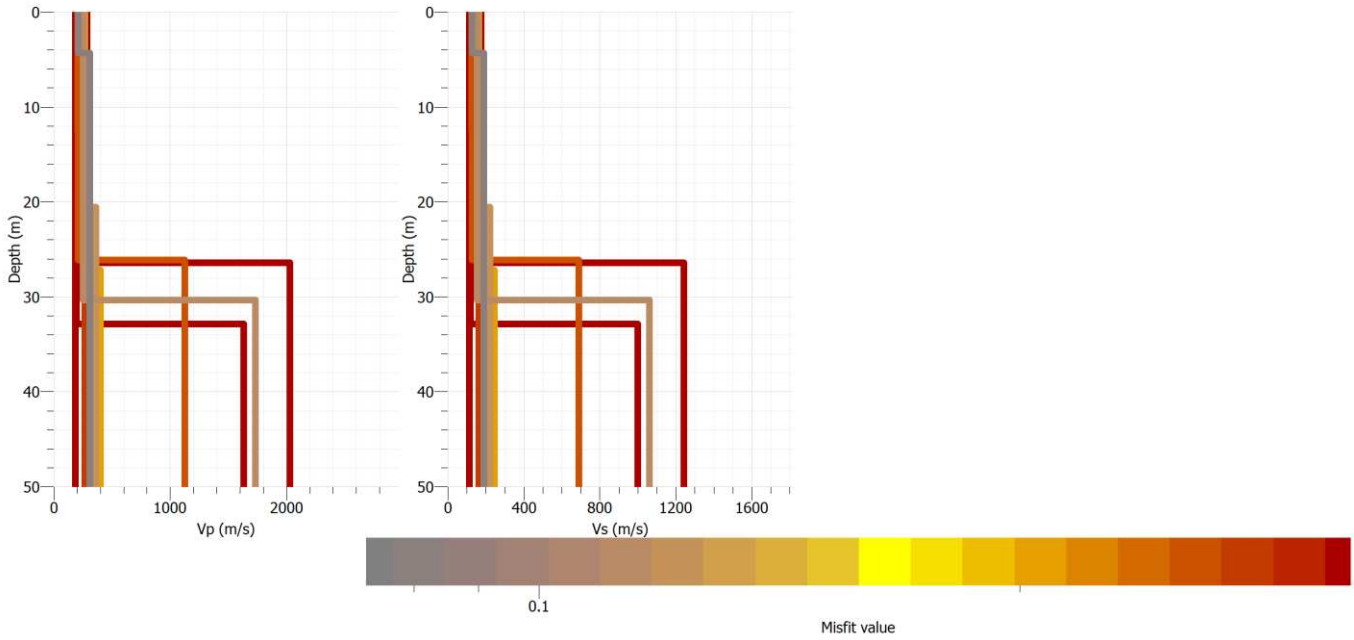

Figure 39: velocity profile of line L7.

6.3. Local seismic response assessment through the passive seismic data acquisitions, using H/V method

An important requirement for the implementation of the H/V method is a good knowledge of engineering seismology combined with background information on local geological conditions supported by geophysical and geotechnical data. In the case we are examining, the report by Georicerche S.R.L (Georicerche, 2024) conducted on the same date as this study (01/29/2024), presents valuable geological data obtained from geotechnical investigations involving 2 drillings at the same site. As illustrated in section 3.5., the method is typically applied in microzonation studies and in investigating the local response of specific sites. In the present document, the application of the H/V technique in assessing local site dominant frequency and subsoil structure assessment is the main focus, whereas other applications regarding local site effects due to dynamic earthquake excitations are not considered.

As mentioned in chapter 4, we used Geopsy software for H/V analysis. To process H/V data using geopsy, the input data consist of the following:

- Three signals: North-South, East-West, and Vertical for the three components at a given receiver.
- Sufficient common time samples for processing.

Before applying the tool, the data may be preprocessed. User have several opportunities for doing this such as;

- The filters or remove trend functions available in the waveform toolbar.
- from a graphic viewer, to verify the windowing and to display the results; as shown in Figure 40.
- similarly to other tools of the software, from the table of metadata, shown in Figure 20. A table allows to view and to edit the header information about signals.

Geopsy H/V toolbox consists of four tabs;

- Time tab
- Processing tab
- Output tab
- Status

As is shown in Figure 41, the time tab allows for defining the duration of the seismic section to be analyzed and setting the width of each time window for H/V amplitude computation. This leads to setting the number of windows by which the chosen length of the data would be divided. It is also possible to choose the filter that applies on each time window. According to the literature reviews on H/V analysis, for computing the H/V amplitudes each horizontal component (EW and NS) can be analyzed separately, but the most common approach is to combine the two horizontal components. There are several methods to do that; In the processing tab of the tool, geopsy allows to choose your desired method of combining the horizontal components of the signal. You can manipulate the filtering type and set smoothing parameters in this tab as well. Moreover, the output tab is dedicated to set frequency sampling parameters and range and the user is also able to manipulate the appearance of the output page. The last tab shows the user the status of the process in moment after the tool runs.

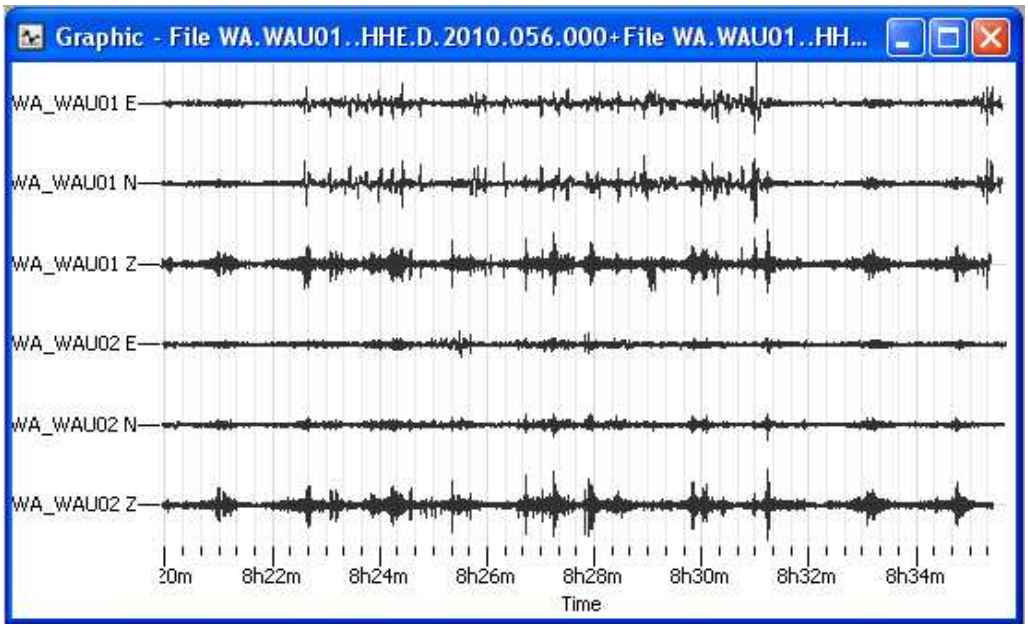

Figure 40: the default graphic viewer(geopsy.org).

In this case study, we have 18 hours of passive recorded data from each sensor, from which we trimmed 20 minutes of the most silent part with the minimum noise, which is from 00:40:00 on the second day of the acquisition to 01:00:00 on the third day, as you see in Figure 41. Based on our prior geological information, the area has soft soil and a flat topography. Hence, we should consider oscillations with frequencies below 10 Hz, as suggested in SESAME TEAM documentation (Teves Costa, 2004). Otherwise, we involve the noise amplitudes in the calculations of H/V ratios.

After starting the tool, selected windows of the waveform are colored in the graphic window, as shown in Figure 42, matching the colors in the H/V curves as shown in Figure 43; i.e., the color of individual H/V curves is the same as the signal windows (Geopsy.org). in Figure 16, the black curve represents H/V geometrically averaged over all colored individual H/V curves. The two dashed lines represent the H/V standard deviation. The grey bar area represents the averaged peak frequency and its standard deviation. The frequency value is at the limit between the dark grey and light grey areas.

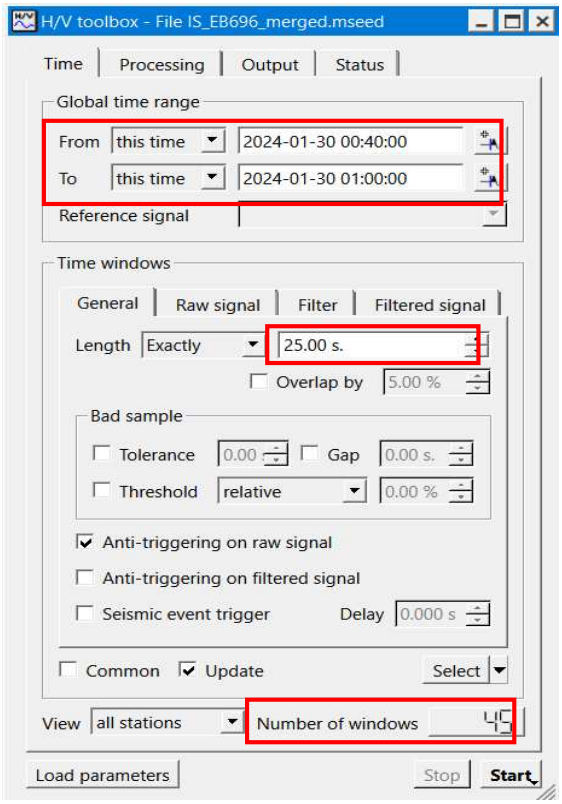

A)

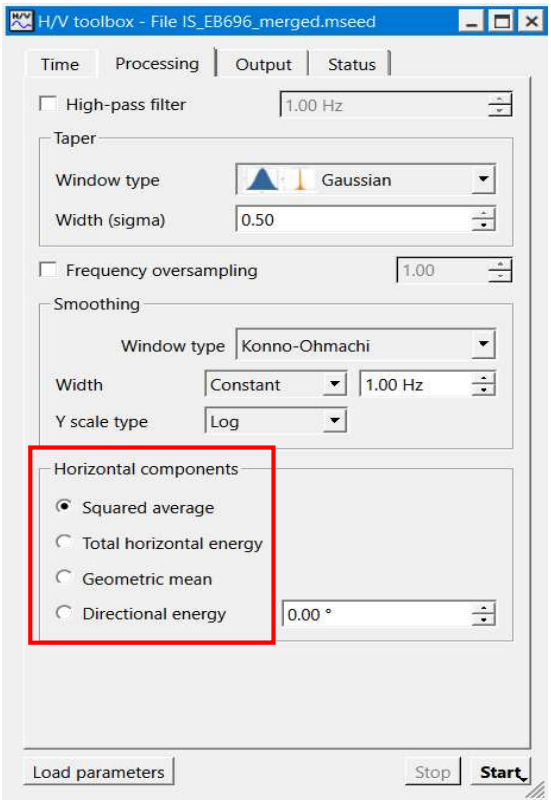

B)

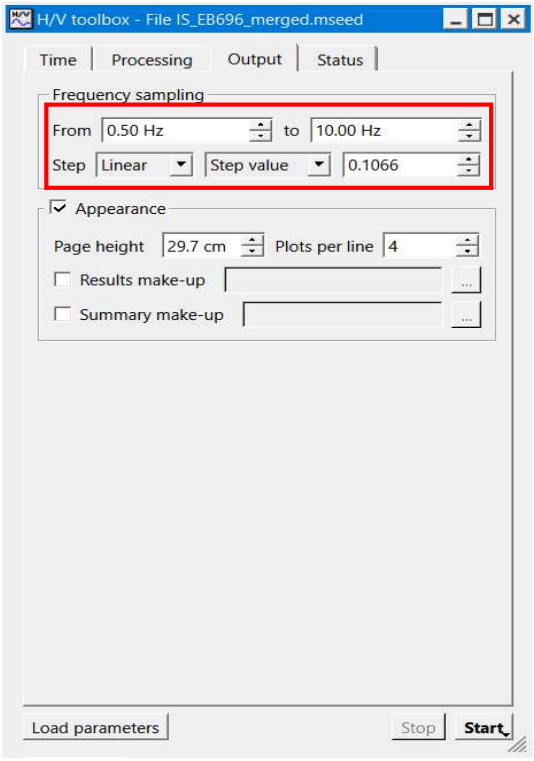

C)

Figure 41: H/V toolbox, A) time tab, B) Processing tab, C) output tab (Geopsy version 3.5.2).

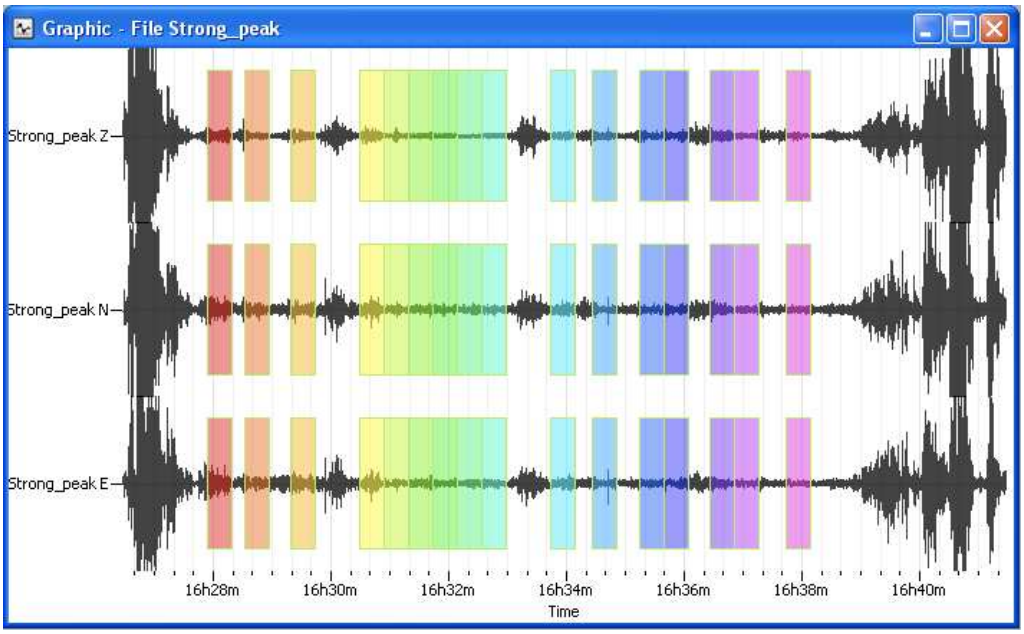

Figure 42: Signal display with colored windows used for computing H/V matching with colors of individual H/V curves presented below (geopsy.org).

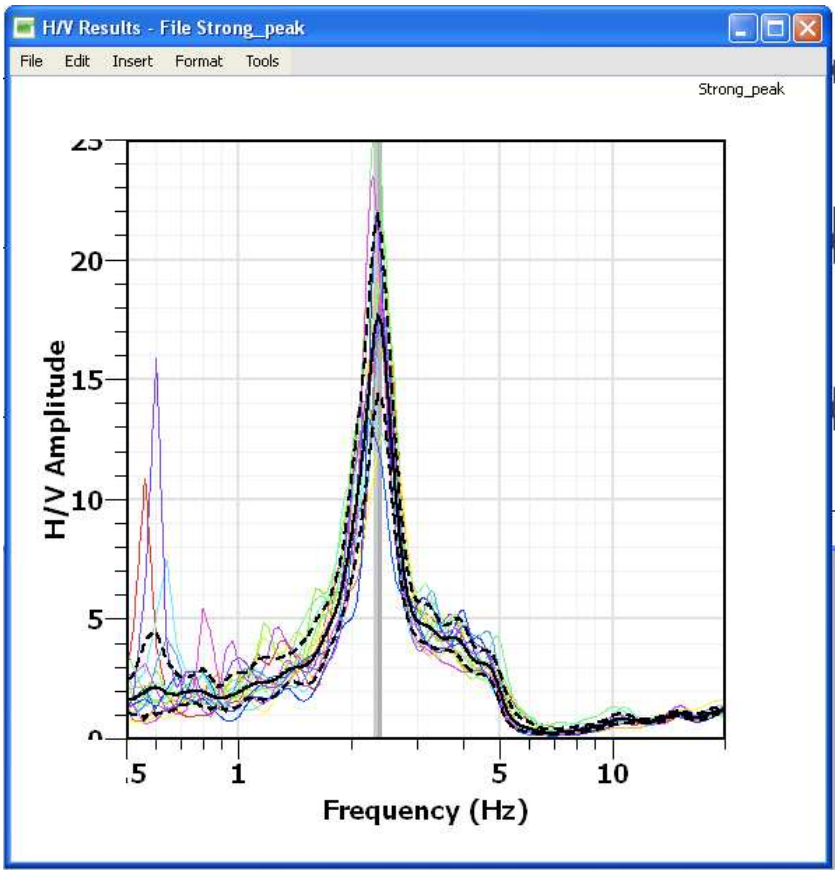

Figure 43: H/V curve example(geopsy.org).

As shown in Figure 18, seven Tritons were installed on the site. The data from the two sensors on the top of the tower were recorded to identify the predominant frequency of the chimney tower, which is not covered in this thesis. Data collected by the other five sensors are used to estimate a site's resonance frequency (f_0) or the predominant frequency of the soil based on ambient noise measurements. We also take advantage of comparing the results of H/V analysis with the results of the velocity modeling in MASW acquisitions to support or reject the hypotheses about the subsoil structure of the site. In the following figures (Figure 45- Figure 49), the results of H/V analysis on the data collected by sensors EB696, EB693, EB694, EB206, and EB695, which are installed on the ground, respectively to their distances from the chimney are shown.

The peak H/V ratios in the results curves are relatively weak. We tried to increase the frequency range to see the ratio values in higher frequencies, as we did for the data from sensor EB696 in Figure 44. For some of the sensors, e.g., EB696, not all of them, the peak is observed in frequencies beyond 10 Hz, but still, the peak is not strong enough to be considered as the predominant frequency of the site, and they might be high-frequency noises. The H/V values recommended by SESAME TEAM (Teves Costa, 2004) to identify f_0, are higher than 3. Hence, in our case, we can use the H/V analysis results combined with the MASW results to gain a view of the site's subsoil structure.

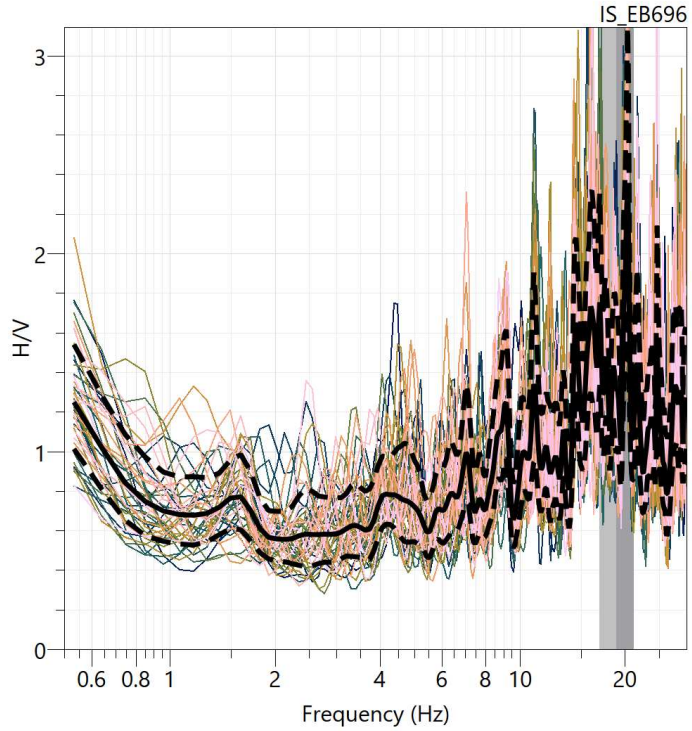

Figure 44: H/V curves, sensor EB696, near the base of the chimney, frequency range up to 30 Hz.

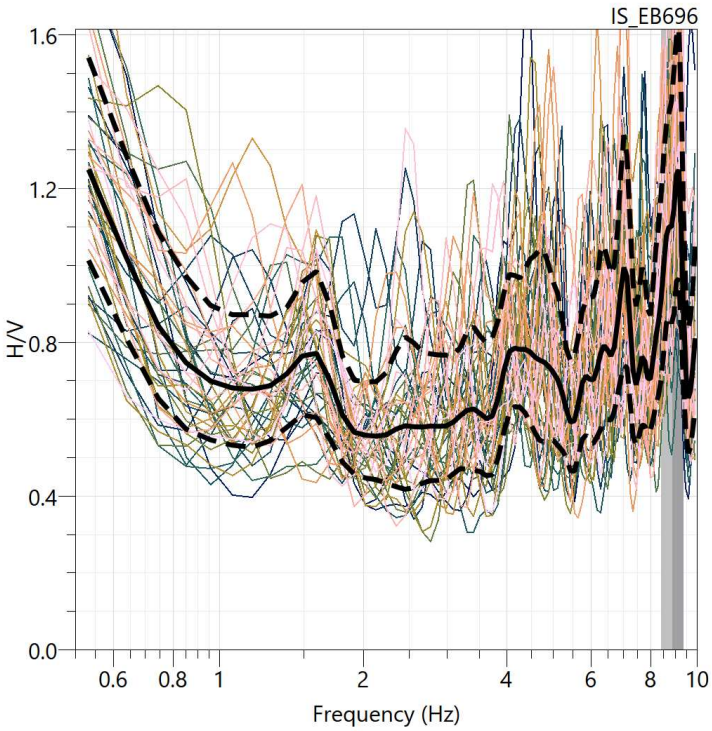

Figure 45: H/V curves, sensor EB696, near the base of the chimney, frequency range up to 10 Hz.

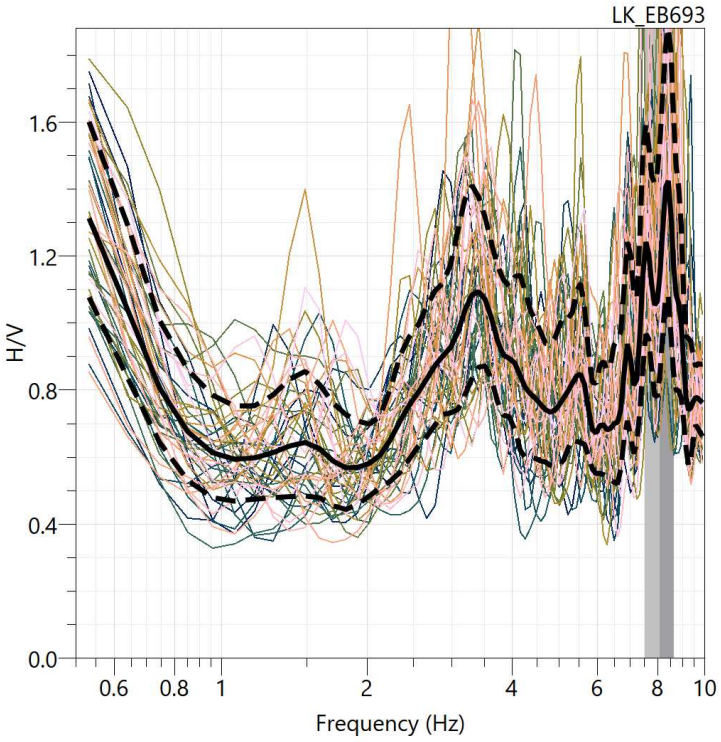

Figure 46: H/V curves, sensor EB693.

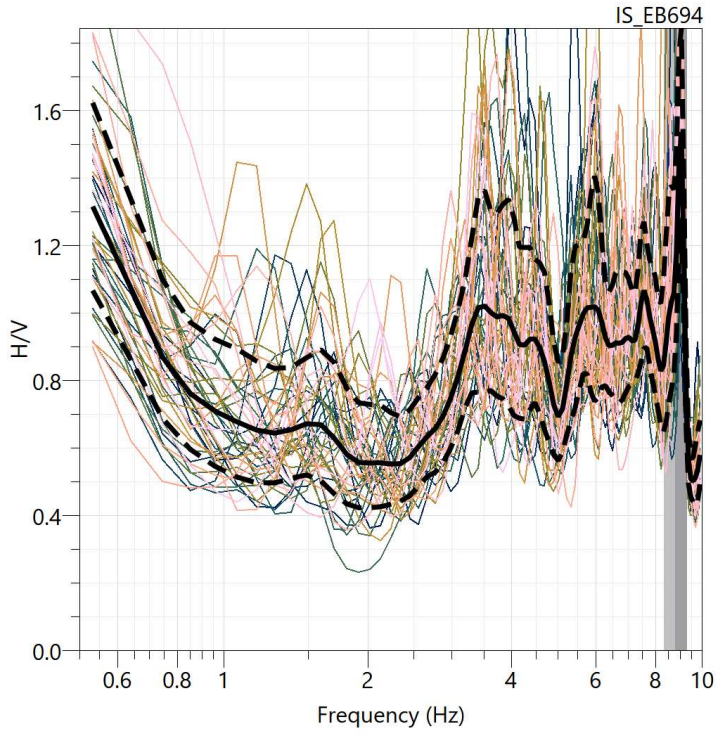

Figure 47: H/V curves, sensor EB694.

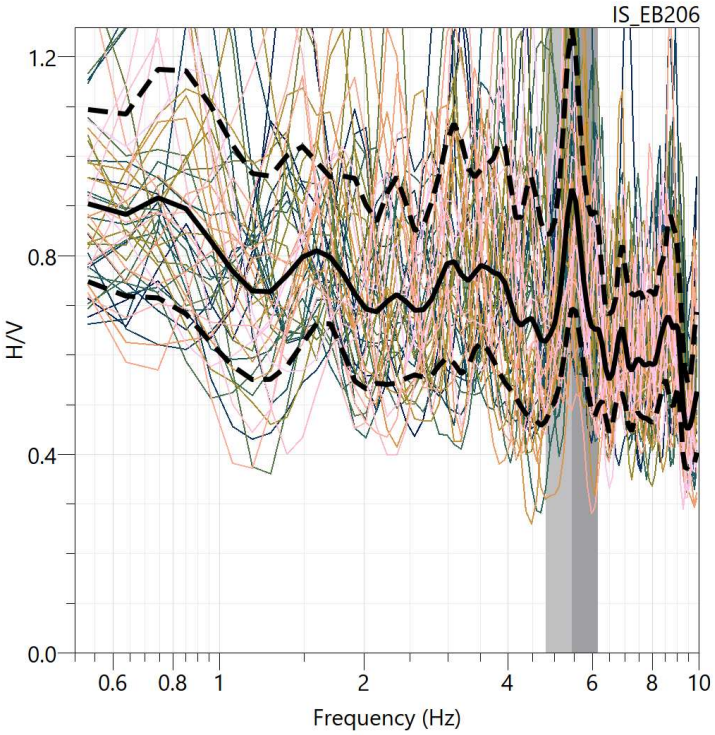

Figure 48: H/V curves, sensor EB206.

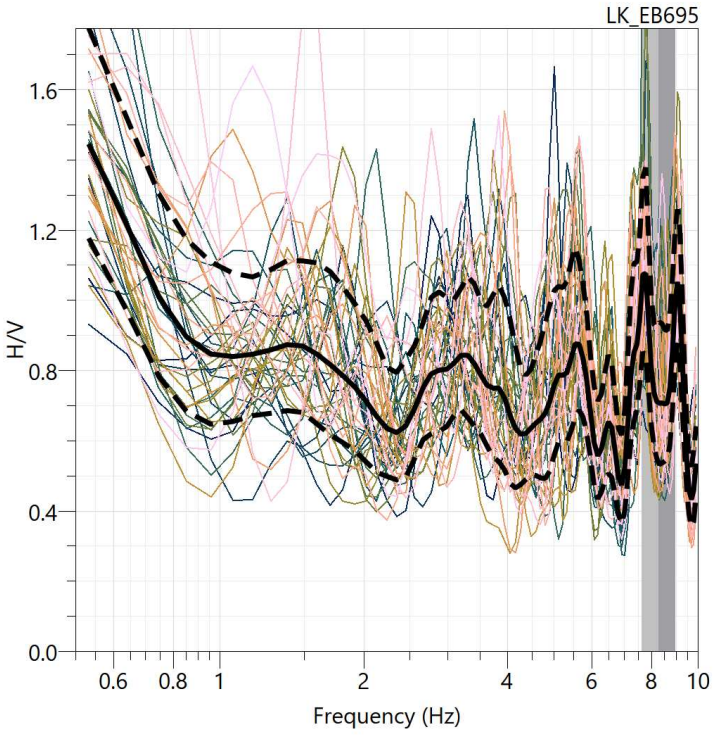

Figure 49: H/V curves, sensor EB695.

7. Results and Conclusions

To give a final view of the active surface wave analysis results, dispersion curves of all the shots on each line of the multi-offset acquisition have been plotted in Figure 50, using Python. To better understand the results, it is good to mention that the total acquisition time for each energization was equal to 3 seconds, and different records were acquired for each array, each corresponding to different distances between the source and the first geophone, generally 3, 6, and 9 meters away. Figure 51 is a plot of the velocity profiles of all 7 lines, resulted from the inversion of the dispersion curves (Figure 50) as illustrated in section 6.2.

At first glance, the dispersion curves (Figure 50) on all the lines have straight patterns, with the exception of line L4, in the phase velocity range of 179 +/-32 m/s. As seen in the velocity profiles of Figure 51, the speed of the S waves is decidedly low, especially in the first 10 meters from the ground level (around 150 m/s) and then gradually increases as an effect of the compaction of the sediments in deeper parts, but settling on average value of around 315 m/s at 50-meter depth. MASW results indicate homogeneity of the media with almost no distinctive anomaly or contrast in elastic moduli. This means the absence of structural complexities in the subsoil and the prior hypothesis of a simple one-layer structure composed of recent and poorly consolidated sediments to a depth of 40 meters is justified.

From the comparison between Figure 50 and Figure 51, it is evident that six out of seven MASW lines present coincident results. The MASW on line L4 shows propagation velocity slightly higher than those of the other lines, including line L3, which is almost perpendicular to L4. L4 and L3 are the nearest lines to the chimney (Figure 18). The most probable reason is that a buried structure in that area affects the collected data in the direction of L4. The high-velocity and high-frequency noise in the MASW results on L4 is not as prominent in the other lines.

The absence of strong impedance anomalies in these 50 m and the very weak nature of the sediments are in perfect agreement with the cores extracted from the drillings (Georicerche, 2024) and of the evidence of the H/V analyses in section 6.3. According to the H/V analysis results, the lack of clear resonant frequencies of the ground in the measurable range between 0.2 Hz and 50 Hz approximately, confirms the lack of strong impedance contrasts in the first tens of meters, as indicated both by the drill cores and by the inversion of the dispersion curves already described. the subsurface materials in this area are homogeneous and do not have distinct layers with varying stiffness or density. Resonance typically arises from the contrast in properties between different layers, causing reflections and standing waves, that is why we cannot report a clear resonance frequency in our results.

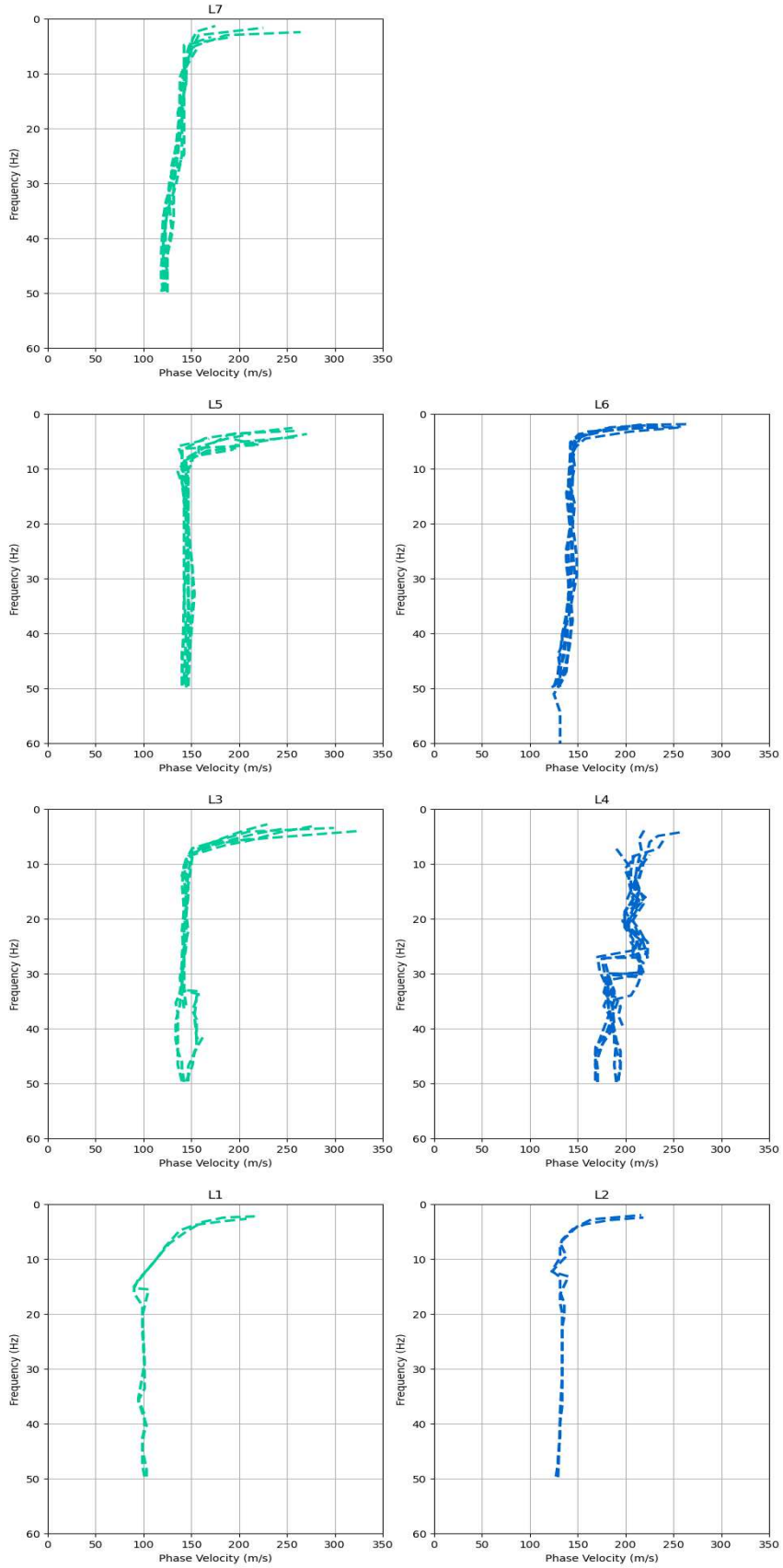

Figure 50: Dispersion curves of all the multi-offset shots, on each line of acquisition in Porto Tolle site (Python).

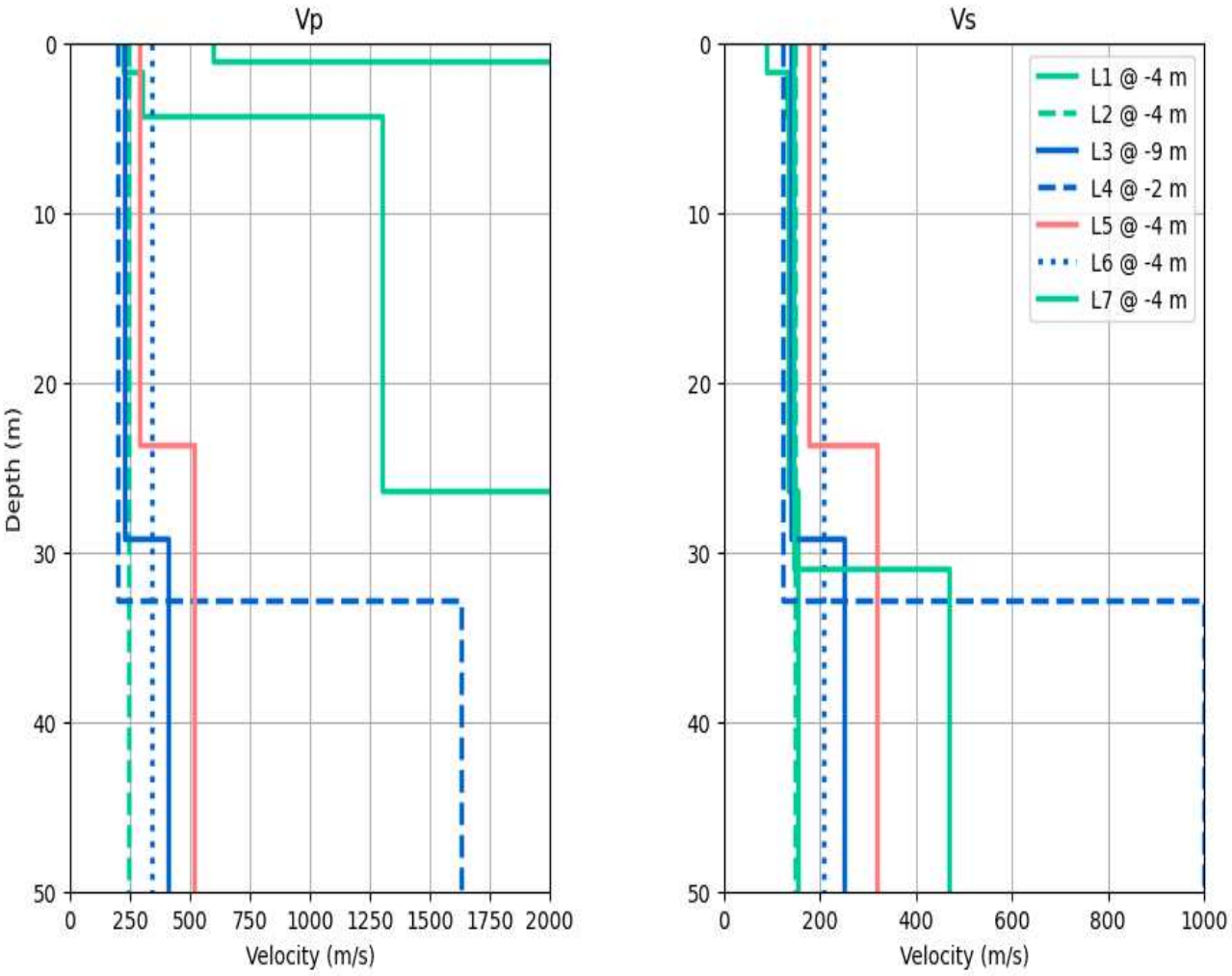

Figure 51: Velocity Profiles of the 7 MASW acquisition lines (Python).

8. Research gaps and future works

Subsequent studies could build upon the findings of this research and analyze further the chimney's dynamic behavior, evaluating the resonance period of this structure to compare with the site period in order to understand possible interactions during potential seismic events. This documentation does not cover these analyses of the data collected by the two sensors installed on top of the structure.

Despite the extensive analysis conducted in this study, several gaps in the current research were identified. As mentioned in the results section, the MASW results on line L4 show propagation speeds higher than those of the other lines. The increase in V_s could be due to various reasons, including the increase in soil compaction, increase in density, or the existence of a buried structural element/object in the area where the data was collected on line L4. It could be worth exploring that area with a geo-radar or checking references on the industrial design of the site to discover potential source and explanation of this anomaly on our data results.

While this research has advanced our understanding of local seismic response of this site, there are still several unanswered questions and areas related to Local Seismic Response Analysis (LSA) that would require further investigation. Expanding the scope of this research to include the dynamic characteristics of the soils could offer a more comprehensive perspective and contribute to seismic hazard estimates.

The current study primarily focused on subsoil structure discovery, leaving the possibility of liquefaction of the materials in the event of an intense seismic event relatively unexplored. Future research should aim to evaluation of the possible liquefaction of the materials in the area.

9. References

Aki, K., and Richards, P.G. 1980. Quantitative seismology: theory and methods.Vol. 1. W.H. Freeman and Co., San Francisco, Calif.

Arslan,U., and Cox, B. R. (2020). *Limits and Ability of the Multichannel Analysis of Surface Waves Method to Detect and Resolve Subsurface Anomalies APPROVED BY SUPERVISING COMMITTEE*.

Bonnefoy-Claudet, S., Köhler, A., Cornou, C., Wathelet, M., & Bard, P.-Y. (2008). Effects of Love Waves on Microtremor H/V Ratio. *Bulletin of the Seismological Society of America*, *98*(1), 288–300. https://doi.org/10.1785/0120070063

Braile, L., 2004. Seismic Wave Demonstrations and Animations. Technical Report. Purdue University.

Chapman, C., 2004, Fundamentals of Seismic Wave Propagation, Cambridge University Press, 29 Jul 2004 - 608 pages

Cox, B. R., Cheng, T., Vantassel, J. P., & Manuel, L. (2021). A statistical representation and frequency-domain window-rejection algorithm for single-station HVSR measurements. *Geophysical Journal International*, *221*(3), 2170–2183. https://doi.org/10.1093/GJI/GGAA119

Dal Moro, G., Pipan, M., & Gabrielli, P. (2007). Rayleigh wave dispersion curve inversion via genetic algorithms and Marginal Posterior Probability Density estimation. *Journal of Applied Geophysics*, *61*(1), 39–55. https://doi.org/10.1016/j.jappgeo.2006.04.002

Enel, 2019, Porto Tolle, from energy to tourism. https://corporate.enel.it/en/stories/articles/2019/07/renaissance-porto-tolle-delta-farm

Foti. (2000). *Multistation Methods for Geotechnical Characterization using Surface Waves*. https://doi.org/10.6092/polito/porto/2497212

Foti, S., Hollender, F., Garofalo, F., Albarello, D., Asten, M., Bard, P. Y., Comina, C., Cornou, C., Cox, B., Di Giulio, G., Forbriger, T., Hayashi, K., Lunedei, E., Martin, A., Mercerat, D., Ohrnberger, M., Poggi, V., Renalier, F., Sicilia, D., & Socco, V. (2018). Guidelines for the good practice of surface wave analysis: a product of the InterPACIFIC project. *Bulletin of Earthquake Engineering*, *16*(6), 2367–2420. https://doi.org/10.1007/s10518-017-0206-7

Foti, S., Lai, C. G., Rix, G. J., & Strobbia, C. (2014). *Surface Wave Methods for Near-Surface Site Characterization*. Taylor & Francis. https://books.google.it/books?id=QmkLBAAAQBAJ

Gabriels, P., Snieder, R. and Nolet, G. 1987. In situ measurements of shear-wave velocity in sediments using higher mode Rayleigh waves. Geophys. Prospect., v.35, pp.187–196.

Geopsy.org, https://www.geopsy.org/wiki/index.php/Welcome_to_GeopsyWiki

Georicerche, 2024, Report della campagna di indagini geosnostiche esequita presso l'ex centrale termoelettrica ENEL s.p.a in comune di Porto Tolle (RO), Provincia di Rovigo, 020/2023/S-V.

Kramer, S.L. 1996. Geotechnical Earthquake Engineering. Prentice-Hall, Inc.,Upper Saddle River, N.J.

Lachet, C., Hatzfeld, D., Bard, Pierre-Yves,Theodulidis, Nikos, Papaioannou, Christos, Savvaidis, Alekos;. 1996, Site effects and microzonation in the city of Thessaloniki (Greece) comparison of different approaches. *Bulletin of the Seismological Society of America* 1996; 86 (6): 1692–1703. doi: https://doi.org/10.1785/BSSA0860061692

Lee, B. J., Kee, S. H., Oh, T., & Kim, Y. Y. (2017). Evaluating the Dynamic Elastic Modulus of Concrete Using Shear-Wave Velocity Measurements. *Advances in Materials Science and Engineering*, *2017*. https://doi.org/10.1155/2017/1651753

Lunitek, https://www.lunitek.it

Nakamura, Y. (1989). *CLEAR IDENTIFICATION OF FUNDAMENTAL IDEA OF NAKAMURA'S TECHNIQUE AND ITS APPLICATIONS*.

Nishida, K. (2017). Ambient seismic wave field. In *Proceedings of the Japan Academy Series B: Physical and Biological Sciences* (Vol. 93, Issue 7, pp. 423–448). Japan Academy. https://doi.org/10.2183/pjab.93.026

Olafsdottir, E. A., Erlingsson, S., & Bessason, B. (2018). Tool for analysis of multichannel analysis of surface waves (MASW) field data and evaluation of shear wave velocity profiles of soils. *Canadian Geotechnical Journal*, *55*(2), 217–233. https://doi.org/10.1139/cgj-2016-0302

Park, C. B. (2005). *MASW – Horizontal Resolution in 2D Shear-Velocity (Vs) Mapping*.

Reynolds, J. M., 2011. An Introduction to Applied and Environmental Geophysics-second edition. WILEY BLACKWELL. p. 170. ISBN 978-0-471-48535-3

Socco, L. V., Jongmans, D., Boiero, D., Stocco, S., Maraschini, M., Tokeshi, K., & Hantz, D. (2010). Geophysical investigation of the Sandalp rock avalanche deposits. *Journal of Applied Geophysics*, *70*(4), 277–291. https://doi.org/10.1016/j.jappgeo.2009.12.005

Socco, L. V., & Strobbia, C. (2004). Surface-wave method for near-surface characterization: a tutorial. *Near Surface Geophysics*, *2*(4), 165–185. https://doi.org/10.3997/1873-0604.2004015

Srinivas, G., K. Goverdhan, C. Narsimhulu, and T. Seshunarayana. 2014. *Estimating Shear Wave Velocity in Drifts Using Multichannel Analysis of Surface Wave (MASW) Technique Case Study from Jammu & Kashmir, India* (Vol. 84).

Teves Costa, P. (2004). *Guidelines for the implementation of the H/V spectral ratio technique on ambient vibrations measurements, processing, and interpretation SESAME European research project WP12-Deliverable D23.12*. http://sesame-fp5.obs.ujf-grenoble.fr/index.htm

Vila,"Types of Hammers". https://www.bobvila.com/articles/1092-types-of-hammers

Wathelet, M., Chatelain, J. L., Cornou, C., Giulio, G. di, Guillier, B., Ohrnberger, M., and Savvaidis, A. 2020. Geopsy: A user-friendly open-source tool set for ambient vibration processing. Seismological Research Letters, 91(3), 1878–1889. https://doi.org/ 10.1785/0220190360 16. Joseph Vantassel.

Yulianto, T., & Yuliyanto, G. (2023). Microtremor data and HVSR method in the kaligarang fault zone Semarang, Indonesia. *Data in Brief*, *49*. https://doi.org/10.1016/j.dib.2023.109428